University of the Pacific Theses and Dissertations

Graduate School

1968

Electrocapillary Studies Of Reversible Charge Transfer V(Iii)/V(Ii) Electrode

Mohammad Ali Akhtar
University of the Pacific

Recommended Citation

Akhtar, Mohammad Ali. (1968). *Electrocapillary Studies Of Reversible Charge Transfer V(Iii)/V(Ii) Electrode*. University of the Pacific, Dissertation. https://scholarlycommons.pacific.edu/uop_etds/2850

ELECTROCAPILLARY STUDIES OF REVERSIBLE CHARGE TRANSFER

V (III) / V (II) ELECTRODE

————————————

A Dissertation

Presented to

The Faculty of the Graduate School

University of the Pacific

————————————

In Partial Fulfillment

of the Requirements for the Degree of

Doctor of Philosophy

————————————

by

Mohammad Ali Akhtar

June 1968

ELECTROCAPILLARY STUDIES OF

REVERSIBLE CHARGE TRANSFER V(III)/V(II) ELECTRODE

Abstract of Dissertation

Electrocapillary equation for an ideal polarized electrode based on Gibb's adsorption equation is appropriately recast into experimentally measurable quantities in order to apply it to a reversible charge transfer electrode.

To calculate the various parameters of the equation developed, experimental details were worked out. For the measurement of Current-time relationship of a single drop, a fast response potentiostat was built by using transistorized chopper stabilized operational amplifiers and precision components in the circuitry with proper compensation for IR-drop in the cell and the electrical double layer capacity. The analysis of I-t curves was done by taking into account the composite nature of the process involved; faradaic and non-faradaic.

V(III)/V(II) reversible charge transfer electrode in absence of any complexing agent was used for its complete reversibility and high cationic adsorption on the electrode.

V(III) and V(II) were prepared in situ in equivalent amounts, by the electrolytic reduction of V(IV). The V(IV) concentration was controlled by photometric titration against standardized potassium permanagate solution.

The drop-time was taken as a measure of interfacial tension, γ, and electrocapillary curves for the pure solvent (1M $HClO_4$ and $0.5M H_2SO_4$) as well as for the varying concentrations of V(III)/ V(II) were drawn by measuring the drop-time from I-t curves and converting it into proper γ units.

The adsorption parameters, such as q^M, $\Gamma_{V,W}^{3+}$, $\Gamma_{V,W}^{2+}$, of the electrical double layer in presence of a charge transfer reaction were calculated.

ACKNOWLEDGEMENTS

TABLE OF CONTENTS

LIST OF TABLES

LIST OF FIGURES

LIST OF FIGURES (continued)

CHAPTER I

INTRODUCTION

The study of the electrical double layer phenomena at
the interfaces composed of a metal in contact with an
electrolyte solution or a molten salt has held the
attention of electrochemists for the last two decades. The
importance of such a venture was primarily felt for two
reasons:

First, the measured values of the fundamental parameters
of electrode kinetics such as rate constants and transfer
coefficients could be strongly dependent on the structure
of the double layer.

Second, the development of several highly sensitive
techniques such as AC polarography, chronopotentiometry,
pulse polarography, and coulostatic analysis brought about
an increasing emphasis on the detection and determination
of trace constituents by electroanalysis. In trace analysis,
adsorption of the constituent sought at the electrode might
become a predominant consideration, for even a fractional
mono-layer could change the electrode response.

If the above phenomena are properly interpreted through
the study of the electrical double layer structure for a
particular system under investigation, the sensitivity of
the electroanalytical method can be extended manyfold and

the precise kinetics and the mechanism of the electrode reaction can be formulated.

Electrical Double Layer is a term used to denote the arrays of charged particles and/or oriented dipoles believed to exist at every material interface. For the present purpose, the term will be restricted to interfaces formed by metals in contact with electrolyte solution.

Models of the double layer go back to Helmholtz (1853)[1] and Quincke (1861)[2]. The first detailed model is due independently to Gouy and Chapman (1913)[3,4], who gave an analysis which is based on the same premises as the Debye-Huckel theory (1923). Agreement between calculated and experimental interfacial tensions was wholly unsatisfactory, for the necessity of considering the compact double layer had been overlooked. Stern[5] modified the Gouy-Chapman model accordingly in 1924, but successful confrontation of the new model with experiment had still to await two advances: one in technique, the other in theory.

It was not realized in early measurements of the double layer capacity with a mercury pool that solutions had to be thoroughly free of the traces of easily absorbed organic impurities. Grahame (1941-1949)[6] perfected the technique and minimized contamination by introducing the use of the dropping mercury electrode in such measurements.

The other advance for successful verification of the

double-layer model of Gouy, Chapman, and Stern was in the nature of an assumption about the compact double layer. Grahame assumed that the compact double-layer capacity is dependent only on the charge on the electrode and not on the electrolyte concentration. This hypothesis was the key to experimental verification of theory (1947, 1954)[6] and provided data for further interpretation of the structure of the compact double layer by Macdonald (1954)[7] and Barlow and Macdonald (1962)[8].

The necessity of considering adsorption effects that can not be interpreted in terms of simple electrostatic interactions of the type analyzed by Gouy and Chapman was briefly alluded to by Gouy (1910)[4]. Stern introduced the concept of specific adsorption and gave it a mathematical formulation based on the Langmuir isotherm (1924)[54]. Grahame (1947) suggested that the specifically adsorbed ions approach the electrode more closely than ions free of specific adsorption.[1,6] He advocated a model of the compact double layer with two planes of closest approach: the inner plane for specifically adsorbed ions and the outer plane for the other ions. The Gouy-Chapman theory is applicable to the region beyond the outer plane, that is, the diffuse double layer. This allows calculation of the amount of specifically adsorbed ions (Grahame and Soderberg-1954) and brings about the important problem of isotherm

assignment.

The qualitative model proposed by Grahame is still considered as the best picture of the electrical double layer.[6,9,10] A schematic diagram is shown in Figure 1.

Briefly, the double layer consists of three main parts: (a) the metallic phase, and (b) an inner layer only a few molecular diameters thick located next to the metal surface on the solutions side of the interface, and (c) an outer, or diffuse layer, which is really a three-dimensional region extending all the way into the bulk of the solution.

In general, the metallic phase bears a net electrical charge on its surface because of an excess or deficit of electrons. This electronic excess or deficit may either be imposed on the metal by means of an external source of electric current, or it may be produced on the metal by the action of a faradaic process. The excess charge resides in so thin a layer in the metallic surface that it may be considered to be effectively two-dimensional. The density of excess electronic charge on the metal surface is denoted by the symbol q^M and is usually expressed in microcoulombs per square centimeter. $q^M < 0$ implies an excess of electrons; $q^M > 0$ implies a deficit.

The inner layer (also called the compact, rigid, Helmholtz, or Stern layer) on the solution side of the
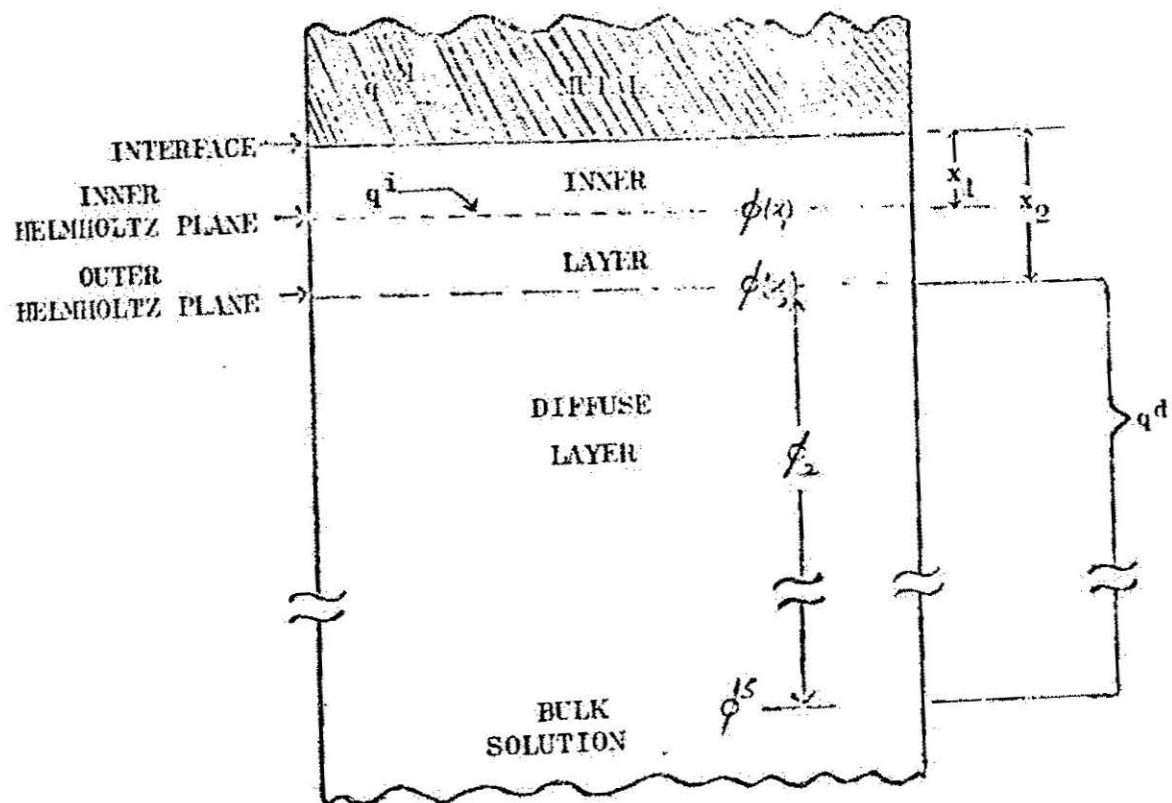
Fig. 1. Schematic Diagram of the Electrical Double Layer

interface contains solvent molecules and sometimes other neutral molecules adsorbed on the surface. In addition, in most electrolyte solutions the inner layer contains a fractional mono-layer of ions which are said to be specifically adsorbed. The locus of the electrical centers of these adsorbed ions is called the inner Helmholtz plane (IHP)[11,12] The electric charge density resulting from this layer is denoted by q^i (usually microcoulombs per square centimeter). The electric potential at the IHP is denoted by $\phi(x_1)$, where the distance of the IHP from the metal surface is given by x_1, which is approximately equal to the radius of the (unsolvated) ion which is specifically adsorbed. The closest the electrical centers of solvated ions can get is a distance $x_2 > x_1$. The imaginary plane passed through the electrical centers of the closest approaching solvated ions is known as the outer Helmholtz plane (OHP) or the Gouy plane[11,12].

In Fig. 2 the small circles containing arrows represent dipoles, the large circles represent specifically adsorbed anions at the IHP and the shaded clusters represent solvated cations at the OHP. It is generally believed that in the case of aqueous electrolyte solutions the closest approaching solvated ions will be separated from the metal surface by a layer of oriented solvent molecules on the metal surface. This is also illustrated in Fig. 2.
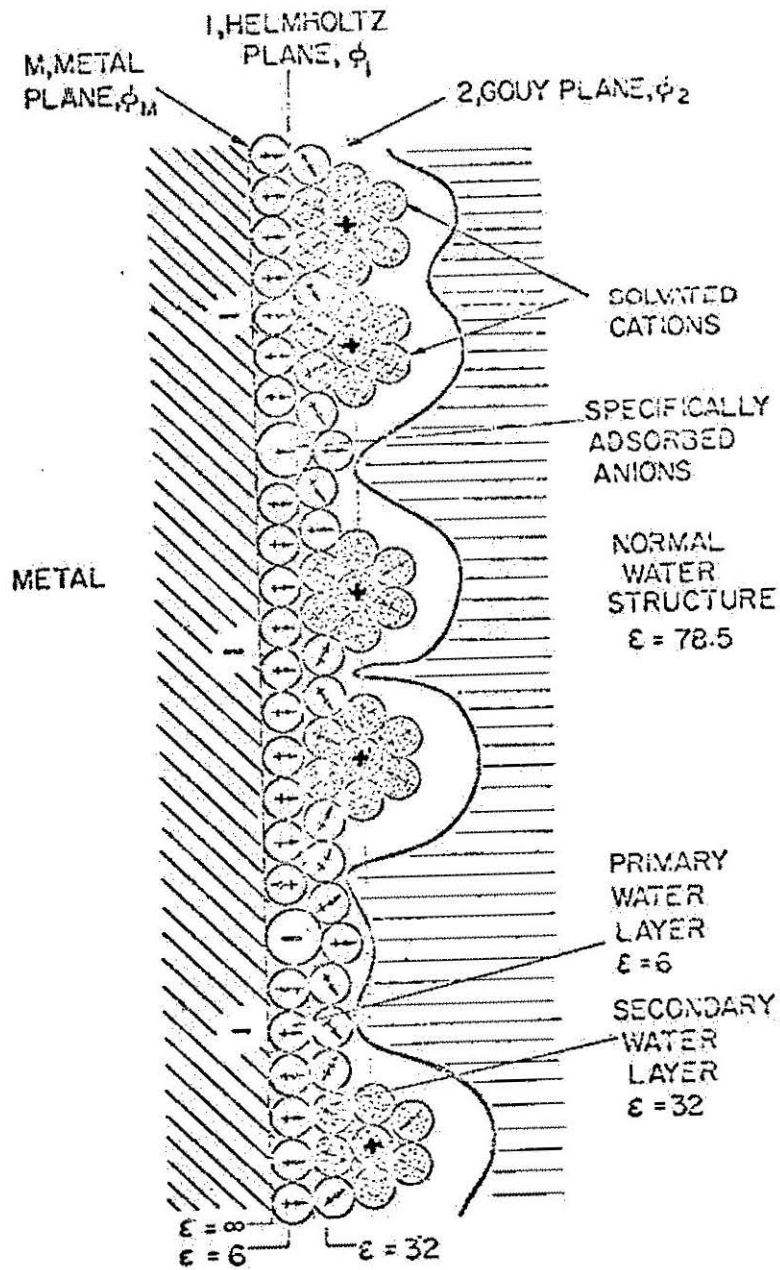
Fig. 2. Solvent adsorption model of the double-layer according to Devanathan, Bockris and Müller. (Proc. Roy. Soc. London A274, 55-1963).

Most of what is known today about the structure and behavior of the electrical double layer has been learned from studies of so-called ideal polarized electrodes[6,13,14]. These are defined as electrodes at which no charge transfer across the metal-solution interface takes place regardless of the potential imposed on the electrode from an outside source of voltage. Strictly speaking, no real electrode system can meet this stringent requirement, but certain systems can approach ideal polarizability very closely, provided the range of imposed electrode potentials is restricted sufficiently. Preeminent among the attainable ideal polarized electrodes is mercury in contact with any of a large variety of carefully deaerated aqueous electrolyte solutions. A familiar example is the dropping mercury electrode (DME).

The various methods in which an ideal polarized electrode is used as a tool for the study of double layer structure are given in Table I[15]. As the electrocapillary method is the most complete and thermodynamically sound method, thermodynamic theory of electrocapillarity will be discussed in the first part of the next section. In the second part of the next section, the application of the above theory to the charge-transfer electrodes will be considered; this part forms the theoretical basis of the present investigation, where an equation for such electrodes

will be derived in terms of experimentally measurable quantities. Little information and experimental data at present is available on this aspect of the electrocapillarity.

TABLE I

Methods for Study of Reactant or
Additive Adsorption at Electrodes

Method	System where Applicable	Principal Limitations	Principal Types of information or Quantities Obtained
Electro-capillary	Liquid metals, amalgams and molten metals	None, except restriction to liquid metal phase	$\Gamma_A, \Gamma_+, \Gamma_-, \gamma^M, \gamma_0^s, \Delta G^\circ, \Theta$ (Γ_A for a neutral species A)
Capacity (Grahame)	Solid and Liquid Metals	(a) Requires electrocapillary or equivalent determination (b) Frequency dependence of capacity	$\Theta, \Gamma_A, \Gamma_+, \Gamma_-, \gamma^s, \Delta G^\circ, C$
Capacity (Hansen)	Solid and Liquid Metals	(a) Frequency dependence of capacity (b) Thermodynamic interpretation not rigorous	Essentially similar to method of Grahame (above) but based on non-thermodynamic deduction of Θ
Radio-isotopes	Solid electrodes with radioactively labelled ions ore molecules	(a) Irreversible adsorption or (b) Cases where back count (C^{14}) can be done; significance of count may be in doubt	Θ; non-equilibrium values of in case (a) or equilibrium in case (b) if electrode maintained in solution.

Table I (continued)

Methods for Study of Reactant or Additive Adsorption at Electrodes

Method	System where Applicable	Principal Limitations	Principal Types of information or Quantities Obtained
D.C. charging determination of H accommodation	Solid Transition Metals	Requires noble metals where can be obtained	Coverage by chemisorbed species deduced by change of H accommodation. Used in electro-catalytic oxidation studies
Spectrophoto-metric	Solid electrodes	(a) Conjugated organic molecules (b) Restricted application to certain organic ions and adsorbents	$\theta, \Gamma, \Delta \bar{G}^{\circ}$
Conductance	Solid and liquid electrodes	(a) Ionic species but not neutral molecules	Speculative and not fully explored; based on changes of ionic concentration
Refractometric	Solid and liquid electrodes	(a) Ionic and neutral molecules where changes in refractive index of adsorbate solutions are significant	Speculative and unexplored; based on changes of concentration

Table I (continued)

Methods for Study of Reactant or
Additive Adsorption at Electrodes

Method	System where Applicable	Principal Limitations	Principal Types of information or Quantities Obtained
A.C. resistance	Solid electrodes	(a) Frequency dependence of impedance measurements (b) Uncertainty of equilibrium thermodynamic significance	Quantitative adsorption parameters not published
Ellipsometric	Smooth solid or liquid electrodes	Requires significant film thickness	Film thickness, based on polarization of reflected radiation

CHAPTER II

THERMODYNAMIC THEORY OF ELECTROCAPILLARITY

Derivation of the Electrocapillary Equation For an Ideal Electrode.

The Gibbs adsorption isotherm for amalgam-electrolyte interface,

$$d\gamma = -\sigma dT - \Gamma_e d\bar{\mu}_e - \sum_i \Gamma_i d\bar{\mu}_i - \sum_j \Gamma_j d\bar{\mu}_j - \sum_k \Gamma_k d\bar{\mu}_k - \sum_k \Gamma_k d\mu_k \quad (1)$$

is a form of electrocapillary equation, where σ is the surface excess of entropy (expressed in $e\,u\,cm^{-2}$); $\Gamma_e, \Gamma_i, \Gamma_j, \Gamma_k$ and Γ_k are the surface excesses of electrons in the metallic phase, of the metal ions in the metallic phase, of the cations, of the anions and of the neutral substances in the solution phase, respectively; $\bar{\mu}_s$ are the electrochemical potentials of the charged species indicated by the subscript; and μ_k is the chemical potential of the neutral substances. However it is not yet in a usable form, because its variables, $\bar{\mu}_e, \bar{\mu}_i, \bar{\mu}_j, \bar{\mu}_k$ cannot be directly measured experimentally. The measurable variables in a laboratory are temperature, pressure, electrode potential and concentrations (activities) of the neutral components. To recast the equation in terms of measurable variables, we must consider in detail the type of cell used in experimental measurements of electrocapillary curves.

(The following method has been adapted from the references (6), (22), (23) and (24).)

Let the complete cell be represented by

$$Cu' \mid M \mid S \mid IN \mid Cu'$$
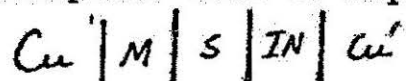
Cu is a metal terminal attached to phase M of the ideal polarized electrode. S is the solution in which indicator electrode IN also dips. IN is reversible to one of the ions of the phase S. Cu' is a metal terminal attached to the metallic phase of the indicator electrode. A potential measuring device is connected across the two terminals. The measured potential difference is defined by the equation

$$E^{\pm} = \phi^{Cu} - \phi^{Cu'} = (\overline{\mu}_e^{Cu'} - \overline{\mu}_e^{Cu})/F \qquad (2)$$

where ϕ^{Cu} and $\phi^{Cu'}$ are the inner potentials of the indicated terminals, $\overline{\mu}_e^{Cu}$ and $\overline{\mu}_e^{Cu'}$ are the electrochemical potentials of the electrons in the two terminals, and E is the potential of the ideal polarized electrode with respect to the indicator electrode[14, 16-18]. E^+ of E^- is used, depending on whether the indicator electrode is reversible to a cation or an anion of the solution respectively.

When two different metals are in contact, the condition of electrochemical equilibrium between them is expressed by the equality of the electrochemical potential of their electrons[17]. Thus, for the contact between terminals and the metallic phase M of the ideal polarized electrode,

$$\overline{\mu}_e^{Cu} = \overline{\mu}_e \qquad (3)$$

Hence the second term of the right side of Eq. (1) becomes

$$\Gamma_e^\prime \, d\bar{\mu}_e^{Cu} \tag{4}$$

For each of the m metals in phase M, we can write a formal dissociation equilibrium expression relating the chemical potential of the metal atoms and the electrochemical potentials of the corresponding metal ions and of the electrons in phase M as

$$d\bar{\mu}_i = d\mu_i - z_i \, d\bar{\mu}_e \tag{5}$$

using equation (3), we get

$$d\bar{\mu}_i = d\mu_i - z_i \, d\bar{\mu}_e^{Cu} \tag{6}$$

Substitution of Eq. (6) into the third term on the right side of Eq. (1), gives

$$\sum_i \Gamma_i^\prime \, d\mu_i - \sum_i \Gamma_i^\prime z_i \, d\bar{\mu}_e^{Cu} \tag{7}$$

Combining expressions (4) and (7), we obtain

$$\sum_i \Gamma_i^\prime \, d\mu_i - \left(\sum_i \Gamma_i^\prime z_i - \Gamma_e^\prime \right) d\bar{\mu}_e^{Cu} \tag{8}$$

By definition, the excess charge density on the metal, q^M, is given by the expression:

$$q^M = \left(\sum_i \Gamma_i^\prime z_i - \Gamma_e^\prime \right) F = - \left(\sum_j \Gamma_j^\prime z_j - \sum_k \Gamma_k^\prime |z_k| \right) F$$

Hence the second and third terms of the Gibbs Adsorption Equation become

$$\sum_i \Gamma_i^\prime \, d\mu_i - \left(\frac{q^M}{F} \right) d\bar{\mu}_e^{Cu} \tag{9}$$

which contains chemical potentials of the metals in phase M instead of electrochemical potentials of the ions in phase M.

To replace the electrochemical potentials of the ions of the solution by chemical potentials of the neutral species, we must first decide what the neutral species, that is, salts are to be.

Suppose that the solution S contains c cationic species and a anionic species. Of the ca different binary salts that could be chosen, we shall select c+a-1 binary salts in the following way.

If the indicator electrode IN is reversible to cation j', we arbitrarily select an anion, say k'. If the indicator electrode is reversible to anion k', we arbitrarily select a cation, say j'. In either case we have selected a binary salt containing ions j' and k'. We shall call this salt the indicator salt. The electrolyte solution is then considered to have been made up by dissolving c+a-2 additional binary salts of which c-1 have anion k' in common with the indicator salt; the remaining a-1 salts have cation j' in common with the indicator salt.

For each salt in S we may write a formal equilibrium

$$\left(C_j\right)_{\nu_{jk}^+} \left(A_k\right)_{\nu_{jk}^-} \rightleftharpoons \nu_{jk}^+ C_j^{z_j} + \nu_{jk}^- A_k^{z_k} \tag{10}$$
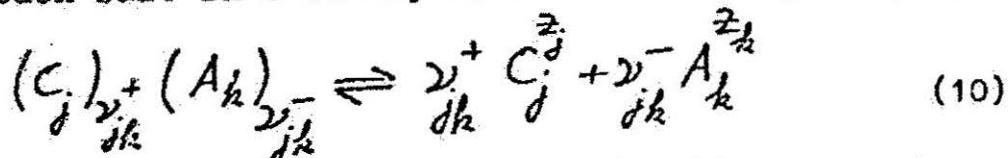
where ν's indicate the number of moles of cations or anions per formula weight of the salt. Since each salt is neutral,

$$\nu_{jk}^+ z_j = \nu_{jk}^- |z_k| \tag{11}$$

Corresponding to each of the above equilibria, there is an equation relating the chemical potentials of the neutral salt to the electrochemical potentials of its constituent ions. Therefore, we have the following c+1-a equations:

$$d\mu_{j'k'} = \nu^+_{j'k'} \, d\bar{\mu}_{j'} + \nu^-_{j'k'} \, d\bar{\mu}_{k'} \tag{12}$$

$$d\mu_{jk'} = \nu^+_{jk'} \, d\bar{\mu}_j + \nu^-_{jk'} \, d\bar{\mu}_{k'} \quad (j \neq j') \tag{13}$$

$$d\mu_{jk} = \nu^+_{jk} \, d\bar{\mu}_{j'} + \nu^-_{jk} \, d\bar{\mu}_k \quad (k \neq k') \tag{14}$$

Equations (12) to (14) allow the electrochemical potentials of the individual ionic species which appear in Eq. (1) to be replaced by the measurable chemical potentials of the neutral salts.

In the j summation of Eq. (1), by substitution for the electrochemical potential of each cation, using Eqs. (12) and (13), we obtain

$$\sum_j \left(\frac{\Gamma_j}{\nu^+_{jk'}} \right) d\mu_{jk'} - \left[\sum_j \Gamma_j \left(\frac{\nu^-_{jk'}}{\nu^+_{jk'}} \right) \right] d\bar{\mu}_{k'}$$

Introduction of Eq. (11) for each salt in the preceding expression, yields

$$\sum_j \left(\frac{\Gamma_j}{\nu^+_{jk'}} \right) d\mu_{jk'} - \left[\sum_j \Gamma_j \left(\frac{z_j}{|z_{k'}|} \right) \right] d\bar{\mu}_{k'} \tag{15}$$

Similarly, substituting Eqs. (12) and (14) into the k summation of Eq. (1) and introducing Eq. (11) for each salt, we get

$$\sum_{k} \left(\frac{\Gamma_k}{\overline{v}_{j'k}} \right) d\mu_{j'k} - \left[\sum_{k} \Gamma_k \left(\frac{|z_k|}{z_{j'}} \right) \right] d\overline{\mu}_{j'} \qquad (16)$$

The electrochemical potentials of all the ions in the solution, except the cation j' and k' of the indicator salt, have been eliminated.

Since the indicator electrode is reversible to an ion of the solution, the electrochemical potential of that ion may be expressed in terms of the electrochemical potential of the electrons in the terminal attached to the indicator electrode and the chemical potentials of the pure substances comprising the indicator electrode. The following equations apply for the indicator electrodes reversible to cation j' (Eq. 17) or to anion k' (Eq. 18):

$$d\overline{\mu}_{j'} = -z_{j'} d\overline{\mu}_e^{cu'} + d\mu_+ \qquad (17)$$
$$= -z_{j'} d\overline{\mu}_e^{cu'} - s_+ dT + v_+ dp$$

$$d\overline{\mu}_{k'} = |z_{k'}| d\overline{\mu}_e^{cu'} + d\mu_- \qquad (18)$$
$$= |z_{k'}| d\overline{\mu}_e^{cu'} - s_- dT + v_- dp$$

The symbols $d\mu_+$ and $d\mu_-$ in Eqs. (17) and (18), respectively, are shorthand notations for the differentials of the chemical potentials of the pure components of the indicator

electrode. Similarly, $\overset{\bullet}{\underset{+}{s}}$, $\overset{\bullet}{\underset{-}{s}}$, $\overset{\bullet}{\underset{+}{v}}$ and $\overset{\bullet}{\underset{-}{v}}$ represent the molar entropies and molar volumes of the pure indicator electrode components.

The actual elimination of the electrochemical potentials of the ions of the indicator salt is divided into two cases depending on whether IN is reversible to the cation j' or the anion k' .

Case I. The indicator electrode is reversible to cation j' . Substitution of Eq. (17) into Eq. (12) and introduction of Eq. (11) yields

$$d\bar{\mu}_{k'} = \left(\frac{1}{\nu^-_{j'k'}}\right)d\mu_{j'k'} + \left|z_{k'}\right|d\bar{\mu}_e^{\,u'} - \left(\frac{\nu^+_{j'k'}}{\nu^-_{j'k'}}\right)d\overset{\bullet}{\mu}_+ \quad (19)$$

Substitution of Eq. (19) into expression (15) eliminates the electrochemical potential of the anion k' and gives

$$\sum_{j \neq j'}\left(\frac{\Gamma_j}{\nu^+_{j'k'}}\right)d\mu_{j k'} - \left[\left(\frac{1}{|z_{k'}|\nu^-_{j'k'}}\right)\sum_{j \neq j'}\Gamma_j z_j\right]d\mu_{j'k'} - \left(\sum_j \Gamma_j z_j\right)d\bar{\mu}_e^{\,u'} + \frac{1}{z_{j'}}\left(\sum_j \Gamma_j z_j\right)d\overset{\bullet}{\mu}_+ \quad (20)$$

Substitution of Eq. (17) into the expression (16) eliminates the electrochemical potential of cation j and gives

$$\sum_{k \neq k'}\left(\frac{\Gamma_k}{\nu^-_{j'k}}\right)d\mu_{j'k} + \left(\frac{\Gamma_{k'}}{\nu^-_{j'k'}}\right)d\mu_{j'k'} + \left(\sum_k \Gamma_k |z_k|\right)d\bar{\mu}_e^{\,u'} - \frac{1}{z_{j'}}\left(\sum_k \Gamma_k |z_k|\right)d\overset{\bullet}{\mu}_+ \quad (21)$$

Adding expression (20) and (21) we get

$$\sum_{j \neq j'}\left(\frac{\Gamma_j}{\nu^+_{j'k'}}\right)d\mu_{j k'} + \sum_{k \neq k'}\left(\frac{\Gamma_k}{\nu^-_{j'k}}\right)d\mu_{j'k}$$

$$+ \left[\left(\frac{\Gamma_{k'}}{\nu^-_{j'k'}}\right) - \left(\frac{1}{|z_{k'}|\nu^-_{j'k'}}\right)\sum_{j \neq j'}\Gamma_j z_j\right]d\mu_{j'k'} \quad (22)$$

$$- \left[\sum_j \Gamma_j z_j - \sum_k \Gamma_k |z_k|\right]d\bar{\mu}_e^{\,u'} + \left[\sum_j \Gamma_j z_j - \sum_k |z_k|\right]\left(\frac{1}{z_{j'}}\right)d\overset{\bullet}{\mu}_+$$

By definition, the charge density on the solution side of the double layer, q^S, is given by

$$q^S = \left(\sum_j \Gamma_j z_j - \sum_k \Gamma_k |z_k| \right) F$$

Hence the expression (22) becomes

$$\sum_{j=j'} \left(\frac{\Gamma_j}{\nu_{jk'}^+} \right) d\mu_{jk'} - \sum_{k \neq k'} \left(\frac{\Gamma_k}{\nu_{j'k}^-} \right) d\mu_{j'k}$$
$$+ \left[\left(\frac{\Gamma_{k'}}{\nu_{j'k'}^-} \right) - \left(\frac{1}{|z_{k'}| \nu_{j'k'}^-} \right) \sum_{j \neq j'} \Gamma_j z_j \right] d\mu_{j'k'} - \left(\frac{q^S}{F} \right) d\bar{\mu}_e^{Cu'} + \left(\frac{q^S}{z_{j'}F} \right) d\mu_+ \quad (23)$$

The electrochemical potentials of all the ions of the solution have now been eliminated from the Gibbs adsorption equation. They have been replaced by the chemical potentials of the c+a-1 neutral salts and two terms involving the excess charge density q^S on the solution side of the double layer.

Case II. The indicator electrode is reversible to anion k'. Proceeding in the same way as in Case I, we obtain the following replacement for the original j and k summations in Eq. (1):

$$\sum_{j=j'} \left(\frac{\Gamma_j}{\nu_{jk'}^+} \right) d\mu_{jk'} + \sum_{k \neq k'} \left(\frac{\Gamma_k}{\nu_{j'k}^-} \right) d\mu_{j'k} + \left[\left(\frac{\Gamma_{j'}}{\nu_{j'k'}^+} \right) - \left(\frac{1}{z_{j'} \nu_{j'k'}^+} \right) \sum_{k \neq k'} \Gamma_k |z_k| \right] d\mu_{j'k'}$$
$$- \left(\frac{q^S}{F} \right) d\bar{\mu}_e^{Cu'} - \left(\frac{q^S}{|z_{k'}|F} \right) d\mu_- \quad (24)$$

All that remains to complete the conversion of the Gibbs adsorption equation into a usable form of electro-capillary equation is to eliminate the three dependent variables by means of the electroneutrality condition and the two Gibbs-Duhem equations.

Substitution of expressions (9) and either (23) or (24) into Eq. (1) yields an equation containing no electrochemical potentials except for those of the electrons in the cell terminals Cu and Cu′. These electrochemical potentials may be eliminated by applying the electroneutrality condition for the whole double layer, that is,

$$-q^s = q^M \tag{25}$$

Using this relationship, and recalling the definition of E^+ and $d\dot{\mu}_+$ $(d\dot{\mu}_+ = -\dot{s}_+ dT + \dot{v}_+ dp)$, we obtain the following for the cation-reversible indicator electrode:

$$d\gamma = -\left[\sigma + \left(\frac{q^M \dot{s}_+}{z_{j'} F}\right)\right] dT + \left(\frac{q^M \dot{v}_+}{z_{j'} F}\right) dp - q^M dE^{\pm} - \sum_{j} \Gamma_j d\mu_j$$
$$- \sum_{j \neq j} \left(\frac{\Gamma_j}{z_{j'}^+}\right) d\mu_{jk} - \sum_{k=k} \left(\frac{\Gamma_k}{\nu_{jk}^-}\right) d\mu_{jk} - \sum_{h} \Gamma_h d\mu_h$$
$$- \left[\left(\frac{\Gamma_{k'}}{z_{jk'}^-}\right) - \left(\frac{1}{|z_{k'}| \nu_{jk'}^-}\right) \sum_{j=j} \Gamma_j z_j\right] d\mu_{jk'} \tag{26}$$

A similar equation is obtained in the case of an anion-reversible indicator electrode, the only differences being that E^- replaces E^+; the coefficient of $d\mu_{jk'}$ is that given in the expression (24), and the terms

$$\left(\frac{q^M \dot{s}_+}{z_{j'} F}\right) \text{ and } \left(\frac{q^M \dot{v}_+}{z_{j'} F}\right)$$

are replaced respectively by

$$-\left(\frac{q^M \dot{s}_-}{|z_{k'}| F}\right) \text{ and } -\left(\frac{q^M \dot{v}_-}{|z_{k'}| F}\right)$$

Equation (26) or its analog still contain two

dependent variables. These may be eliminated through the
Gibbs-Duhem equations for the metallic and solution phases.
For the metallic phase, the Gibbs-Duhem equation is

$$-S_M dT + v_M dp - \sum_i x_i d\mu_i = 0 \tag{27}$$

Here S_M and v_M denote the mean molar entropy and mean molar
volume, respectively, of the homogeneous portion of phase
M, and x_i's are the mole fractions of the metals there. T
is the absolute temperature and p is the pressure inside
homogeneous phase M.

We select arbitrarily one of the metals i' of phase M
and designate it the reference metal. Then we solve Eq.
(27) for $d\mu_{i'}$ and substitute for it in either form of Eq. (26).
Similarly, the Gibbs-Duhem equation for the solution phase
is

$$-s_s dT - v_s dp - x_{j'k'} d\mu_{j'k'} - \sum_{j \neq j'} x_{jk'} d\mu_{jk'}$$

$$- \sum_{k \neq k'} x_{j'k} d\mu_{j'k} - \sum_h x_h d\mu_h = 0 \tag{28}$$

where s_s and v_s are the mean molar entropy and volume of
homogeneous solution S and the x's are the mole fractions
of the indicated components in the bulk of the solution.
We select arbitrarily one of the neutral components h as
a reference substance in the solution; usually h is the
solvent. We solve Eq. (28) for $d\mu_h$ and substitute for it
in either form of Eq. (26). The result of the two

substitutions just described is the following equation:

$$d\gamma = -\left\{ \left[\sigma - \left(\frac{S_M}{x_{2'}}\right)\Gamma_{2'} - \left(\frac{S_s}{x_{h'}}\right)\Gamma_{h'} \right] + \left(\frac{q^M S_+^\circ}{z_{j'}F}\right) \right\} dT$$

$$- \left\{ \left[\left(\frac{v_M}{x_{2'}}\right)\Gamma_{2'} + \left(\frac{v_s}{x_{h'}}\right)\Gamma_{h'} \right] - \left(\frac{q^M v_+^\circ}{z_{j'}F}\right) \right\} dp$$

$$- q^M dE^+ - \sum_{i \neq 2'}\left[\Gamma_i - \left(\frac{x_i}{x_{2'}}\right)\Gamma_{2'} \right] d\mu_i$$

$$- \sum_{j \neq j'}\left[\left(\frac{\Gamma_j}{v_{jh'}^+}\right) - \left(\frac{x_{jh'}}{x_{h'}}\right)\Gamma_{h'} \right] d\mu_{jh'}$$

$$- \sum_{h \neq h'}\left[\left(\frac{\Gamma_h}{v_{jh}^-}\right) - \left(\frac{x_{jh}}{x_{h'}}\right)\Gamma_{h'} \right] d\mu_{j'h}$$

$$- \sum_{h \neq h'}\left[\Gamma_h - \left(\frac{x_h}{x_{h'}}\right)\Gamma_{h'} \right] d\mu_h$$

$$- \left\{ \left[\left(\frac{\Gamma_{h'}}{v_{j'h'}^-}\right) - \left(\frac{x_{j'h'}}{x_{h'}}\right)\Gamma_{h'} \right] - \left(\frac{1}{|z_{h'}|v_{j'h'}^-}\right)\sum_{j \neq j'}\Gamma_j z_j \right\} d\mu_{j'h'}$$

(29)

A similar equation would be obtained for the case of an anion-reversible indicator electrode (Case II).

Equation (29) is a correct, complete version of the

Gibbs adsorption equation for the electrical double layer
at an ideal polarized electrode. This is the ELECTRO-
CAPILLARY EQUATION. It is expressed in terms of m+c+a+b
independent variables, each of which is an experimentally
measurable quantity. One of these variables, $E^{\pm}$, is the
potential difference imposed across the terminals of the
cell. $E^{\pm}$ is the additional electrical variable which
characterizes the condition of the electrostatic
equilibrium of an ideal polarized electrode as compared
with the thermodynamic equilibrium in nernstian sense,
which would have one less degree of freedom.

Although Eq. (29) is a correct electrocapillary
equation, it appears cumbersome. Its form can be simplified
by introducing the concept of relative surface excess or
relative adsorption of the components, the relative surface
excess of entropy and the relative thickness of the
interphase[19, 20].

The adsorption of a neutral molecular species $h \neq h'$
relative to that of the reference component h' is defined by
the equation

$$\Gamma_{h h'} = \Gamma_h - \left(\frac{x_h}{x_{h'}} \right) \Gamma_{h'}' \tag{30}$$

When the relative surface excess $\Gamma_{h h'}$ of component h is zero,
we have

$$\left(\frac{\Gamma_h}{\Gamma_{h'}} \right) = \left(\frac{x_h}{x_{h'}} \right) = \left(\frac{C_h}{C_{h'}} \right) \tag{31}$$

where the c's are molar concentrations in the homogeneous
solution.

Positive relative surface excess implies

$$\left(\frac{\Gamma_h}{\Gamma_{h'}}\right) > \left(\frac{x_h}{x_{h'}}\right) = \left(\frac{c_h}{c_{h'}}\right) \tag{32}$$

whereas a negative $\Gamma_{hh'}$ implies

$$\left(\frac{\Gamma_h}{\Gamma_{h'}}\right) < \left(\frac{x_h}{x_{h'}}\right) = \left(\frac{c_h}{c_{h'}}\right) \tag{33}$$

Equations (31) to (33) show that the relative surface excess $\Gamma_{hh'}$
is not a direct measure of the amount of component h
adsorbed but is rather a measure of the amount by which
the adsorption of h exceeds that of the arbitrarily chosen
reference component h'. Thus $\Gamma_{hh'}=0$ does not imply the
absence of adsorbed h; rather it implies that components
h and h' are both adsorbed in the same ratio as their bulk
concentrations. Positive $\Gamma_{hh'}$ implies that the electrical
double layer is relatively richer in component h than is
the bulk of the solution; negative $\Gamma_{hh'}$ implies the double
layer is relatively poorer in h. Note that the relative
surface excess of the reference component $\Gamma_{h'h'} = 0$.

The relative surface excess of the charged components
are defined in a similar way. In phase M the adsorption
of metallic ions of species i is taken relative to that of
ions of the reference species i'. Thus

$$\Gamma_{ii'} = \Gamma_i - \left(\frac{x_i}{x_{i'}}\right)\Gamma_{i'} \tag{34}$$

The adsorption of the cations and anions of the solution is taken relative to that of the neutral reference component h'. Thus

$$\Gamma_{jh'} = \Gamma_j - \nu_{jh'}^+ \left(\frac{x_{jh'}}{x_{h'}} \right) \Gamma_{h'} \tag{35}$$

and

$$\Gamma_{kh'} = \Gamma_k - \nu_{jk}^- \left(\frac{x_{jk}}{x_{h'}} \right) \Gamma_{h'} \tag{36}$$

We note that the multiplier of $\left(\dfrac{\Gamma_{h'}}{x_{h'}} \right)$ in Eqs. (35) and (36) is not just the mole fraction of the salt furnishing the ion but is the mole fraction of that of the salt multiplied by the number of moles of ion contained in one formula weight of the salt. In other words, the multiplier is the mole fraction of the ion in the homogeneous solution S. In keeping with this idea, we define the relative surface excess of the ions of the indicator salt by the equations

$$\Gamma_{j'h'} = \Gamma_{j'} - \sum_k \nu_{j'k}^+ \left(\frac{x_{j'k}}{x_{h'}} \right) \Gamma_{h'} \tag{37}$$

and

$$\Gamma_{k'h'} = \Gamma_{k'} - \sum_j \nu_{jk'}^- \left(\frac{x_{jk'}}{x_{h'}} \right) \Gamma_{h'} \tag{38}$$

The summations are required in Eqs. (37) and (38) because

cation j' is furnished by all a of the different salts supplying the different anions, whereas the anion k' is supplied by all c of the salts supplying the different cations. Similarly, the relative surface excess of the electrons of the metallic phase may be defined by

$$\Gamma'_{ei'} = \Gamma'_e - \sum_i z_i \left(\frac{x_i}{x_{i'}} \right) \Gamma'_i \qquad (39)$$

The relative surface excess of entropy $\sigma_{i'h'}$, is defined by the equation

$$\sigma_{i'h'} = \sigma - \left(\frac{S_M}{x_{i'}} \right) \Gamma'_i - \left(\frac{S_S}{x_{h'}} \right) \Gamma'_h \qquad (40)$$

To obtain the relative thickness of the interphase we rearrange the coefficient of dp,

$$- \left[\left(\frac{v_M}{x_{i'}} \right) \Gamma'_i + \left(\frac{v_S}{x_{h'}} \right) \Gamma'_h \right] = - \left[\left(\frac{\Gamma'_i}{C_{i'}} \right) + \left(\frac{\Gamma'_h}{C_{h'}} \right) \right]$$

where c_i' and c_h' represent the concentrations of components i' and h' in moles per c.c. in homogeneous phases M and S, respectively. Let τ be the thickness of the interphase. It can be proved by considering the dimensions of the electrical double layer that

$$\tau_{i'h'} = - \left[\left(\frac{\Gamma'_i}{C_{i'}} \right) + \left(\frac{\Gamma'_k}{C_{h'}} \right) \right]$$

where $\tau_{i'h'}$ is the relative thickness of the interphase.

Substitution of Eqs. (30), (34), to (38), and (40) into Eq. (29) yields the following final forms of the

electrocapillary equation for an ideal polarized electrode.

Case I.   Indicator electrode reversible to cation j':

$$d\gamma = -\left[\sigma_{i\hbar'} + \left(\frac{q^M \varsigma_+}{z_{j'}F}\right)\right]dT + \left[\tau_{i\hbar'} + \left(\frac{q^M \dot{v}_+}{z_{j'}F}\right)\right]dp$$

$$- q^M dE^+ - \sum_{i \neq i'} \Gamma_{i i'} d\mu_i - \sum_{j \neq j'}\left(\frac{\Gamma_{j i'}}{v^+_{j k'}}\right)d\mu_{j k'}$$

$$- \sum_{k \neq k'}\left(\frac{\Gamma_{k i'}}{v^-_{j' k}}\right)d\mu_{j k} - \sum_{h \neq i'}\Gamma_{h i'} d\mu_h$$

$$- \left[\left(\frac{\Gamma_{j' i'}}{v^+_{j' k'}}\right) - \left(\frac{1}{z_{j'}v^+_{j' k'}}\right)\sum_{k=k'}\Gamma_{k i'}|z_k|\right]d\mu_{j' k'} \quad (41)$$

Case II.   Indicator electrode reversible to anion k':

$$d\gamma = -\left[\sigma_{i\hbar'} - \left(\frac{q^M \varsigma_-}{|z_{k'}|F}\right)\right]dT + \left[\tau_{i\hbar'} - \left(\frac{q^M \dot{v}_-}{|z_{k'}|F}\right)\right]dp$$

$$- q^M dE^- - \sum_{i \neq i'}\Gamma_{i i'} d\mu_i - \sum_{j \neq j'}\left(\frac{\Gamma_{j i'}}{v^+_{j k'}}\right)d\mu_{j k'}$$

$$- \sum_{k \neq k'}\left(\frac{\Gamma_{k i'}}{v^-_{j' k}}\right)d\mu_{j k} - \sum_{h \neq i'}\Gamma_{h i'} d\mu_h$$

$$- \left[\left(\frac{\Gamma_{j' i'}}{v^+_{j' k'}}\right) - \left(\frac{1}{z_{j'}v^+_{j' k'}}\right)\sum_{k=k'}\Gamma_{k i'}|z_k|\right]d\mu_{j' k'} \quad (42)$$

Derivation of Electrocapillary Equation for a Charge-
Transfer Electrode.

The theory of the electrocapillary curve for revers-
ible charge transfer electrodes was treated first by

Grahame and Whitney[24] (1962) and was considered in somewhat more detail by Mohilner[22] (1962). Little experimental data on this aspect of electrocapillarity has been reported yet. Koenig and co-workers[25] have reported recently on the mercury-mercurous ion electrode.

From the standpoint of the thermodynamic theory of electrocapillarity, the only essential difference between an ideal polarized electrode and an electrode at which a reversible charge transfer process takes place is that the latter electrode has one less degree of freedom than it would have were it ideally polarizable (i.e., one less independent variable). We consider the charge-transfer half reaction in general as

$$O + ne = R \tag{43}$$

where O represents the oxidized form of the couple, n is the number of electrons involved, and R represents the reduced form of the couple. Let both substances O and R be cations.

The condition of charge-transfer equilibrium for the half reaction is given by an equation expressing the equality of the electrochemical potentials of reactants and products[10], that is

$$\bar{\mu}_O + n\bar{\mu}_e = \bar{\mu}_R \tag{44}$$

Let the cell be represented by

$$Cu \mid M \mid S \mid IN \mid Cu'$$

where Cu and Cu$'$ are two copper terminals. Cu is connected to the test electrode M, and Cu$'$ to the indicator electrode, IN. The indicator electrode is reversible to one type of ions of the solution S. Solution S contains the redox couple. Let the indicator ion be represented by k$'$. Ignoring the solvent of the solution S for simplicity, we can represent the cell as:

$$Cu \;\Big|\; M \;\Big|\; (O, \overset{S}{R}, k') \;\Big|\; \overset{IN}{\underset{k'}{\text{with ions}}} \;\Big|\; Cu'$$
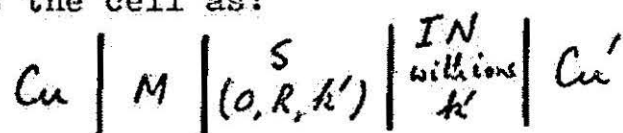
The chemical potentials of the neutral salts Ok$'$, Rk$'$ can be written as

$$\mu_{Ok'} = \nu_{Ok'}^{+} \, \bar{\mu}_{O} + \nu_{Ok'}^{-} \, \bar{\mu}_{k'} \tag{45}$$

and

$$\mu_{Rk'} = \nu_{Rk'}^{+} \, \bar{\mu}_{R} + \nu_{Rk'}^{-} \, \bar{\mu}_{k'} \tag{46}$$

From Eqs. (44), (45) and (46), on taking differentials, we get

$$\left(\frac{1}{\nu_{Ok'}^{+}}\right) d\mu_{Ok'} - \left(\frac{\nu_{Ok'}^{-}}{\nu_{Ok'}^{+}}\right) d\bar{\mu}_{k'} + n \, d\bar{\mu}_{e} = \left(\frac{1}{\nu_{Rk'}^{+}}\right) d\mu_{Rk'} - \left(\frac{\nu_{Rk'}^{-}}{\nu_{Rk'}^{+}}\right) d\bar{\mu}_{k'} \tag{47}$$

As Cu is in contact with M, the metallic phase of the reversible charge-transfer electrode, therefore

$$d\bar{\mu}_{e} = d\bar{\mu}_{e}^{Cu} \tag{48}$$

Further, as $h' - |z_{k'}|e = k_0'$, where $|z_{k'}|$ is the magnitude of the charge on anion k' and k'_0 is the neutral species, therefore

$$d\bar{\mu}_{k'} - |z_{k'}|d\bar{\mu}_e = d\mu_{k_0'} \tag{49}$$

At constant temperature and pressure, $d\mu_{k_0'}$ is constant. Therefore the equation (49) becomes

$$d\bar{\mu}_{k'} = |z_{k'}|d\bar{\mu}_e \tag{50}$$

In terms of the electrons in terminal Cu', Eq. (50) can be written as

$$d\bar{\mu}_{k'} = |z_{k'}|d\bar{\mu}_e^{Cu'} \tag{51}$$

Owing to the electroneutrality of salts, we have

$$\left(\frac{\nu_{ok'}^-}{\nu_{ok'}^+}\right) = \frac{z_0}{|z_{k'}|} \quad \text{and} \quad \left(\frac{\nu_{Rk'}^-}{\nu_{Rk'}^+}\right) = \frac{z_R}{|z_{k'}|} \tag{52}$$

where z_0 and z_R represent the ionic charges of the substances O and R, respectively.

From the half-reaction (43), it follows that

$$z_0 - z_R = n \tag{53}$$

Substitution of Eqs. (48), (51), (52) and (53) is Eq. (47),

gives

$$\left(\frac{1}{\nu_{Ok'}^+}\right)d\mu_{Ok'} - n\left(d\bar{\mu}_e^{Cu'} - d\bar{\mu}_e^{Cu}\right) = \left(\frac{1}{\nu_{Rk'}^+}\right)d\mu_{Rk'} \tag{54}$$

By definition[19],

$$FE^- = \left(\bar{\mu}_e^{Cu'} - \bar{\mu}_e^{Cu}\right) \tag{55}$$

Substitution of Eq. (55) in Eq. (54), yields

$$\left(\frac{1}{\nu_{Ok'}^+}\right)d\mu_{Ok'} - nFdE^- = \left(\frac{1}{\nu_{Rk'}^+}\right)d\mu_{Rk'} \tag{56}$$

Reverting to Eqs. (41) and (42), at constant temperature, pressure and the composition of the electrode, the equations are reduced to:

Case I. Indicator electrode is reversible to cation j':

$$d\gamma = -q^M dE^+ - \sum_{k=k'}\left(\frac{\Gamma_{kk'}}{\nu_{jk}^-}\right)d\mu_{jk} \tag{57}$$

Case II. Indicator electrode is reversible to anion k':

$$d\gamma = -q^M dE^- - \sum_{j \neq j'}\left(\frac{\Gamma_{jk'}}{\nu_{jk'}^+}\right)d\mu_{jk'} \tag{58}$$

Applying the Eq. (58) to the charge-transfer reaction (43) and considering the case when there is no solvent present, we get

$$dr = -q^M dE^- - \left(\frac{\Gamma'_{Ox'}}{\nu^+_{Ox'}}\right) d\mu_{Ox'} - \left(\frac{\Gamma'_{Rh'}}{\nu^+_{Rh'}}\right) d\mu_{Rh'}$$

(59)

Eq. (59) is only applicable when the electrode is ideally polarized. For a charge-transfer electrode, the above equation must have one less independent variable.

Substitution of Eq. (56) in Eq. (59) gives the required equation:

$$dr = -q^M dE^- - \left(\frac{\Gamma'_{Ox'}}{\nu^+_{Ox'}}\right) d\mu_{Ox'} - \left(\frac{\Gamma'_{Rh'}}{\nu^+_{Ox'}}\right) d\mu_{Ox'} - nF\Gamma'_{Rh'} dE^-$$

or

$$dr = -(q^M - nF\Gamma'_{Rh'}) dE^- - \left(\frac{1}{\nu^+_{Ox'}}\right)(\Gamma'_{Ox'} + \Gamma'_{Rh'}) d\mu_{Ox'}$$

(60)

The above equation (60) was applied experimentally to study the electrocapillary properties of V^{3+}/V^{2+} reversible charge-transfer electrode in the present investigation. Non-complexing solvents, 1M $HClO_4$ and 0.5M H_2SO_4 were used. The metallic phase was $Hg(DME)$. The systems can be represented as follows:

(1) V^{3+}/V^{2+} in 1M $HClO_4$

$$Cu \left| Hg \right| V^{3+}, V^{2+}, H^+, ClO_4^- \left| IN \right| Cu'$$
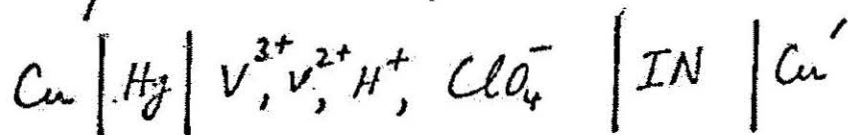
$$dr = -(q^M - \Gamma_{V,w}^{2+} F) dE^- - (\Gamma_{V,w}^{2+} + \Gamma_{V,w}^{3+}) d\mu_{V(ClO_4)_3} - \Gamma_{H,w}^+ d\mu_{HClO_4}$$

(61)

(2) V^{3+}/V^{2+} in $0.5M$ H_2SO_4

$$Cu \,\Big|\, Hg \,\Big|\, V^{3+}, V^{2+}, H^+, SO_4^{2-} \,\Big|\, IN \,\Big|\, Cu'$$
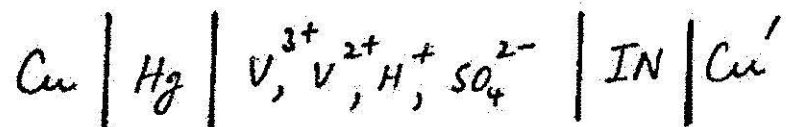
$$d\gamma = -(q^M - \Gamma_{V,\omega}^{2+} F)dE - \frac{1}{2}\left[\Gamma_{V,\omega}^{2+} + \Gamma_{V,\omega}^{3+}\right]d\mu_{V_2(SO_4)_3} - \frac{1}{2}\Gamma_{H,\omega}^+ d\mu_{H_2SO_4} \tag{62}$$

V^{3+}/V^{2+} electrode was selected for two reasons:

(i)   It was a simple redox reaction which could be studied at Hg.

(ii) The double-layer effects were expected to be very prominent due to the possible adsorption of cations.

CHAPTER III

EXPERIMENTAL

Theory of Experimental Measurements.

In Eqs. (61) and (62), the unknown quantities are

$$\gamma, \; q^M, \; \Gamma_{V, \omega}^{2+} \; and \; \Gamma_{V, \omega}^{3+}$$

These quantities can be determined experimintally as follows:

i) <u>Determination of γ</u>: Drop-time variation with varying potential has recently been taken as a measure of γ as a function of potential[26]. Thus

$$\gamma = k.t$$

where t is drop-time of DME at a particular potential, γ is the interfacial tension at that potential, k is a constant depending upon the dimensions of the capillary used in the DME and the pressure of the Hg column.

In order to convert t into γ, the value of k is required. The value of k can be determined from γ_{ECM} (interfacial tension at the electrocapillary maximun) for a particular electrolyte. In the case of 1M $HClO_4$ solution γ_{ECM} is 420 dynes per cm.[27] Therefore we can write

$$k = \frac{420}{t_{ECM}}$$

The k value for 1M $HClO_4$ in the present investigation

proved to be 1.086×10^2 dynes sec.$^{-1}$ cm.$^{-1}$; t_{ECM} was 3.87 seconds. The same value is applicable for 0.5M H_2SO_4 solution.

The drop-time in the test electrolytes was determined as a function of applied potential from the current-time plots of the recorder by calculating the time between two adjacent peaks for each applied potential (shown in Fig. 3).

Drop-time vs. Potential plots were converted into the corresponding γ vs. Potential plots by multiplying t-values by the factor 1.086×10^2.

ii) <u>Determination of q^M</u>: The charging current I_c of the double-layer can be determined by constant potential amperometry of a single drop by using a fast scan recorder. The mathematical relationship between q^M (excess of charge density cm^{-2}) and I_c can be derived as follows:

Let us suppose that

a = surface area of the electrode (cm^2)

v = volume of the electrode (cm^3)

m = mass-flow rate of Hg (gm sec^{-1})

q^M = excess charge density on metal (μcoulombs cm^{-2})

r = radius of electrode (cm)

ρ_{Hg} = density of mercury (gm cm^{-3})
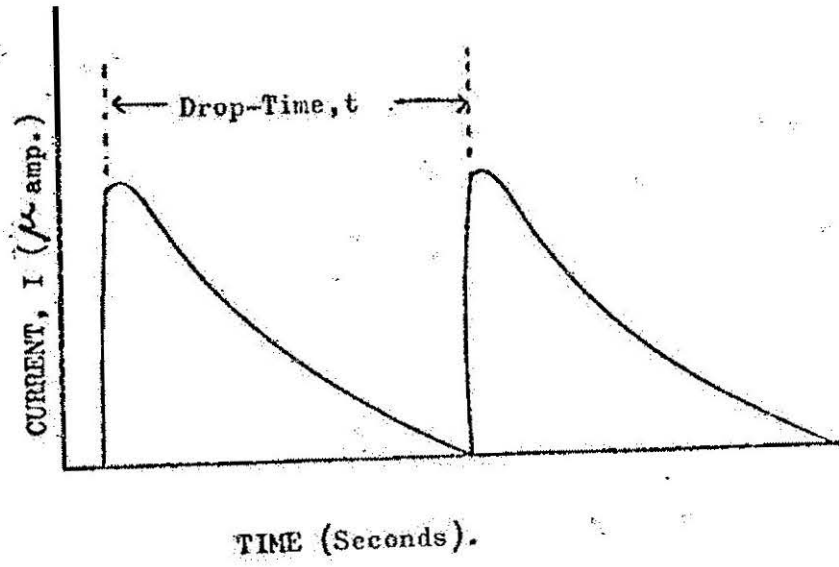
FIG. 3.   Drop-Time Measurement

Then

$$\text{mass a drop} = mt, \qquad \rho_{Hg} = \frac{m \cdot t}{V}$$

and

$$V = \frac{mt}{\rho_{Hg}} = \frac{4}{3} \pi r^3$$

or

$$r = \frac{3^{\frac{1}{3}} \cdot m^{\frac{1}{3}} \cdot t^{\frac{1}{3}}}{4^{\frac{1}{3}} \cdot \pi^{\frac{1}{3}} \cdot \rho_{Hg}^{\frac{1}{3}}} \tag{63}$$

As

$$a = 4\pi r^2$$

Therefore

$$\frac{da}{dt} = 8\pi r \cdot \frac{dr}{dt} \tag{64}$$

From Eq. (63) on taking differentials, we obtain

$$\frac{dr}{dt} = \left(\frac{1}{3}\right) \frac{3^{\frac{1}{3}} \cdot m^{\frac{1}{3}}}{4^{\frac{1}{3}} \cdot \pi^{\frac{1}{3}} \cdot \rho_{Hg}^{\frac{1}{3}}} \cdot t^{-\frac{2}{3}}$$

or

$$r \cdot \frac{dr}{dt} = \left(\frac{1}{3}\right) \frac{3^{\frac{2}{3}} \cdot m^{\frac{2}{3}}}{4^{\frac{2}{3}} \cdot \pi^{\frac{2}{3}} \cdot \rho_{Hg}^{\frac{2}{3}}} \cdot t^{-\frac{1}{3}} \tag{65}$$

Substitution of Eq. (65) into Eq. (64) gives

$$\frac{da}{dt} = 8\pi \left(\frac{1}{3}\right) \frac{3^{\frac{2}{3}} \cdot m^{\frac{2}{3}}}{4^{\frac{2}{3}} \cdot \pi^{\frac{2}{3}} \cdot \rho_{Hg}^{\frac{2}{3}}} \cdot t^{-\frac{1}{3}}$$

By definition, charging current, I_c, is given by

$$I_c = q^M \cdot \frac{da}{dt} \quad (\mu \text{ coulomb sec}^{-1}).$$

Therefore

$$I_c = q^M \left[8\pi \left(\tfrac{1}{3}\right) \frac{3^{\frac{2}{3}} \cdot m^{\frac{2}{3}}}{4^{\frac{2}{3}} \cdot \pi^{\frac{2}{3}} \cdot \rho_{Hg}^{\frac{2}{3}}} \cdot t^{-\frac{1}{3}} \right] \tag{66}$$

Butler and Meehan have shown that the total current passing through a cell is a composite of currents of various processes taking place in the cell.[28] They have given the following relationship:

$$I_{total} = At^{-\frac{1}{3}} + Bt^{\frac{1}{6}} - B't^{\frac{1}{6}} - ct^{\frac{2}{3}} \tag{67}$$

where $At^{-1/3}$ is the charging current of the double-layer, $Bt^{1/6}$ is the Faradaic current due to diffusion controlled anodic dissolution, $B't^{1/6}$ is the current due to cathodic deposition and $Ct^{2/3}$ is current due to activation controlled hydrogen evolution.

In the present study, as we are dealing only with the charging of the double-layer and a faradaic process (charge-transfer reaction), therefore we will consider only the first two terms on the right-hand side of the Eq. (67). That is

$$I_{total} = At^{-\frac{1}{3}} + Bt^{\frac{1}{6}}$$

or

$$It^{\frac{1}{3}} = A + Bt^{\frac{1}{2}} \tag{68}$$

Eq. (68) is the equation of a straight line. Therefore on

plotting $It^{1/3}$ against $t^{1/2}$, the intercept on $It^{1/3}$ axis gives the value of A.

We know that the charging current component of the total current through the cell is given by the relation

$$I_c = A\,t^{-\frac{1}{3}}$$

Thus, from Eqs. (66) and (68), we get

$$I_c = At^{-\frac{1}{3}} = q^M(3.22)\left(\frac{m}{\ell_{Hg}}\right)^{\frac{2}{3}} t^{-\frac{1}{3}}$$

or

$$q^M = \frac{A}{3.22}\left(\frac{\ell_{Hg}}{m}\right)^{\frac{2}{3}}$$

$$(69)$$

I at different potentials can be experimentally determined. Hence q^M for the corresponding potentials can be calculated therefrom.

iii) <u>Determination of Surface Excesses, $\Gamma_{V,\omega}^{2+}$ and $\Gamma_{V,\omega}^{3+}$.</u>

At constant p, T, and μ_s', the equations (61) and (62) are reduced to

$$\left(\frac{\partial \gamma}{\partial E^-}\right)_{T,p,\mu_s} = -q^M + F\,\Gamma_{V,\omega}^{2+}$$

$$(70)$$

From the slope of the $\gamma - E^-$ curve (electrocapillary curve) at a particular potential and from the value of q^M at that potential, we can find the corresponding value

of $\Gamma_{V,\omega}^{2+}$.

At constant E^- and μ_{acid}, the equations are further reduced to

$$\left(\frac{\partial \gamma}{\partial \mu}\right)_{E^-, \mu_{acid}}^{V(ClO_4)_3} = -\left(\Gamma_{V,\omega}^{2+} + \Gamma_{V,\omega}^{3+}\right)$$

and

$$\left(\frac{\partial \gamma}{\partial \mu_{V_2(SO_4)_3}}\right)_{E^-, \mu_{acid}} = -\frac{1}{2}\left(\Gamma_{V,\omega}^{2+} + \Gamma_{V,\omega}^{3+}\right)$$

As

$$d\mu_{salt} = RT\, d\ln a_{salt}$$

therefore, in terms of a_{salt} (activity), the equations can be rewritten as

$$\frac{1}{RT}\left(\frac{\partial \gamma}{\partial \ln a_{V(ClO_4)_3}}\right)_{E^-, \mu_{acid}} = -\left(\Gamma_{V,\omega}^{2+} + \Gamma_{V,\omega}^{3+}\right) \tag{71}$$

and

$$\frac{1}{RT}\left(\frac{\partial \gamma}{\partial \ln a_{V_2(SO_4)_3}}\right)_{E^-, \mu_{acid}} = -\frac{1}{2}\left(\Gamma_{V,\omega}^{2+} + \Gamma_{V,\omega}^{2+}\right) \tag{72}$$

From the slope of γ-ln a_{salt} plot, we can find the values of the right-hand expression of Eqs. (71) and (72) at a particular a_{salt} and a particular E^-. Knowing the value of $\Gamma_{V,\omega}^{2+}$ under the same conditions from Eq. (70), the value of $\Gamma_{V,\omega}^{3+}$ can be determined.

Instrumentation.

(i) Polarograph: As a polarograph with a good response time, a wide stability margin and low signal to noise ratio at very low concentrations was not available in this laboratory, a circuit according to Booman and Holbrook using transistorized operational amplifiers was built.[29] The circuit diagram is shown in Fig. 4 . The transistor operational amplifiers used were Model DY-2460A amplifiers and Model DY-2416A-M4, +1 Gain, plug-in units made by DYMEC, a division of the Hewlett-Packard Co. (Palo Alto, California). The power supplies for each amplifier were self-contained. The required amplifier arrangement for the circuit was obtained by a simple modification in connections as suggested by the authors in the above reference.

The power supplies, PS-1 and PS-2 were inexpensive Isoply units, Model AS 12-40, made by Elcor (Falls Church, Va.)

The building blocks of the circuit are shown in dotted spaces of the Fig. 4. Amplifier A-5 forms the scanner unit, A-2 is in the mode of a Voltage Follower. There is a choice of current amplifying units. Current can be measured at the output of A-3 or A-4, both act as current amplifiers. The original paper discusses the
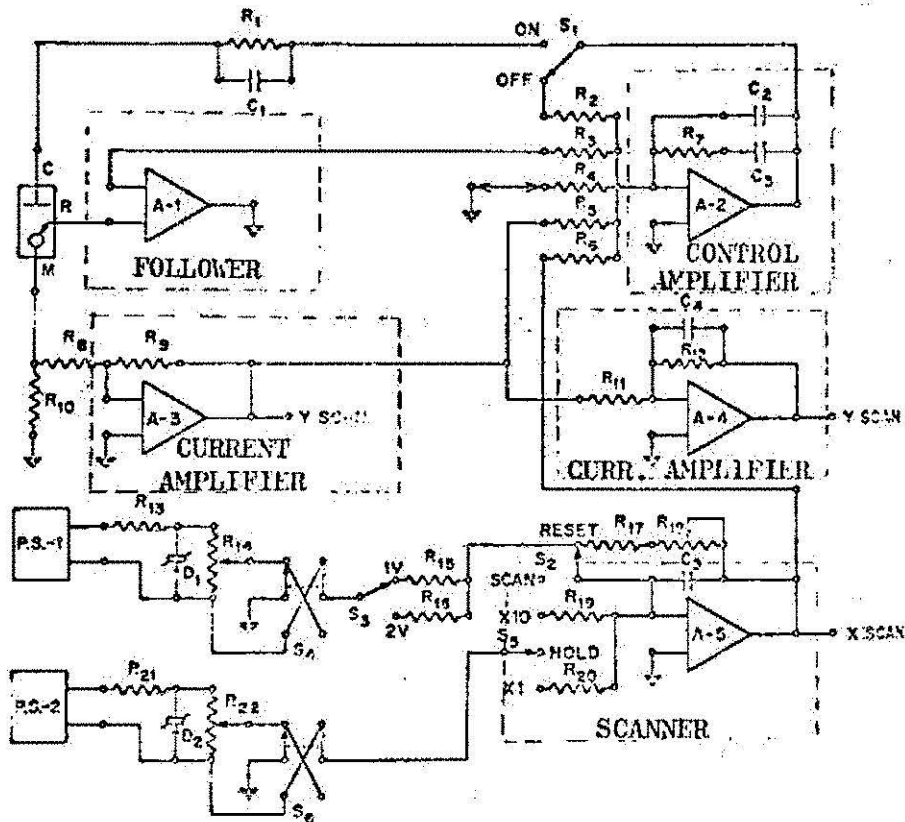
Fig. 4 Polarograph circuit.

$C_1 = 0.5$ fd, $C_2 = 34$ pf., $C_3 = 520$ pf., C_4 = 0.25 fd., D_1, D_2 = INI1522A Zener Diodes, R_1 = 50K, R_3, R_5, R_8, R_9 = 10K, R_7 = 9.5 megohms, R_{10} = 10K, R_{12} = 560 K., R_{13}, R_{21} = 160 ohms, R_{14} = 1 K, 10 turn pot, R_{15}, R_{17} = 100 K, R_{16} = 200 K, R_{18} = 50 K trim pot, R_{19} = 10 megohms, R_{20} = 100 megohms, R_{22} = 10 K, 3 turn pot, S_1, S_2, S_3 = SPST Switch, S_4, S_6 = DPDT Switch, S_5 = SPDT Switch.

complete analysis of the circuit.

(ii) <u>Cell</u>: A three-compartment cell with fritted glass
partitions was designed for the present purpose. An all
glass DME (dropping mercury electrode) was fitted into the
central compartment and sealed from atmospheric air with a
mercury seal. The glass DME was considered an important
factor in measurement of the drop-time more accurately and
with better reproducibility as pointed out by Barradas and
French.[30] The design used three fritted glass-bubblers,
one in each of the three compartments, for passing nitrogen
through the solution during deaeration. Arrangement was
also made to pass nitrogen over the solutions in all three
compartments during the time of making measurements. In
one of the outer compartments an H-shaped SCE (saturated
calomel electrode) was placed, while in the other outer
compartment an auxiliary or counter platinum electrode was
fitted. Both SCE and the counter electrode had standard
taper joints fitting into the air-tight male joints of the
covers of the outer compartments.

The fritted glass partitions between the compartments
were considered necessary in order to avoid as much as
possible the contamination of the solution in the central
compartment, especially from the SCE compartment.

A complete sketch of the cell is given in the Fig. 5.

GAS INLET →

GAS INLET

GAS INLET

← TO MERCURY RESERVOIR

← DROPPING MERCURY ELECTRODE

GAS INLET

GAS INLET

← GAS INLET

COUNTER
ELECTRODE →

Hg SEAL

GAS OUTLET TO
WATER BUBBLER

SATURATED
CALOMEL
ELECTRODE

GAS OUTLET
TO WATER
BUBBLER

GAS OUTLET
TO WATER
BUBBLER

FRIT GLASS
GAS BUBBLER

FRIT GLASS
PARTITION

FRIT GLASS
PARTITION
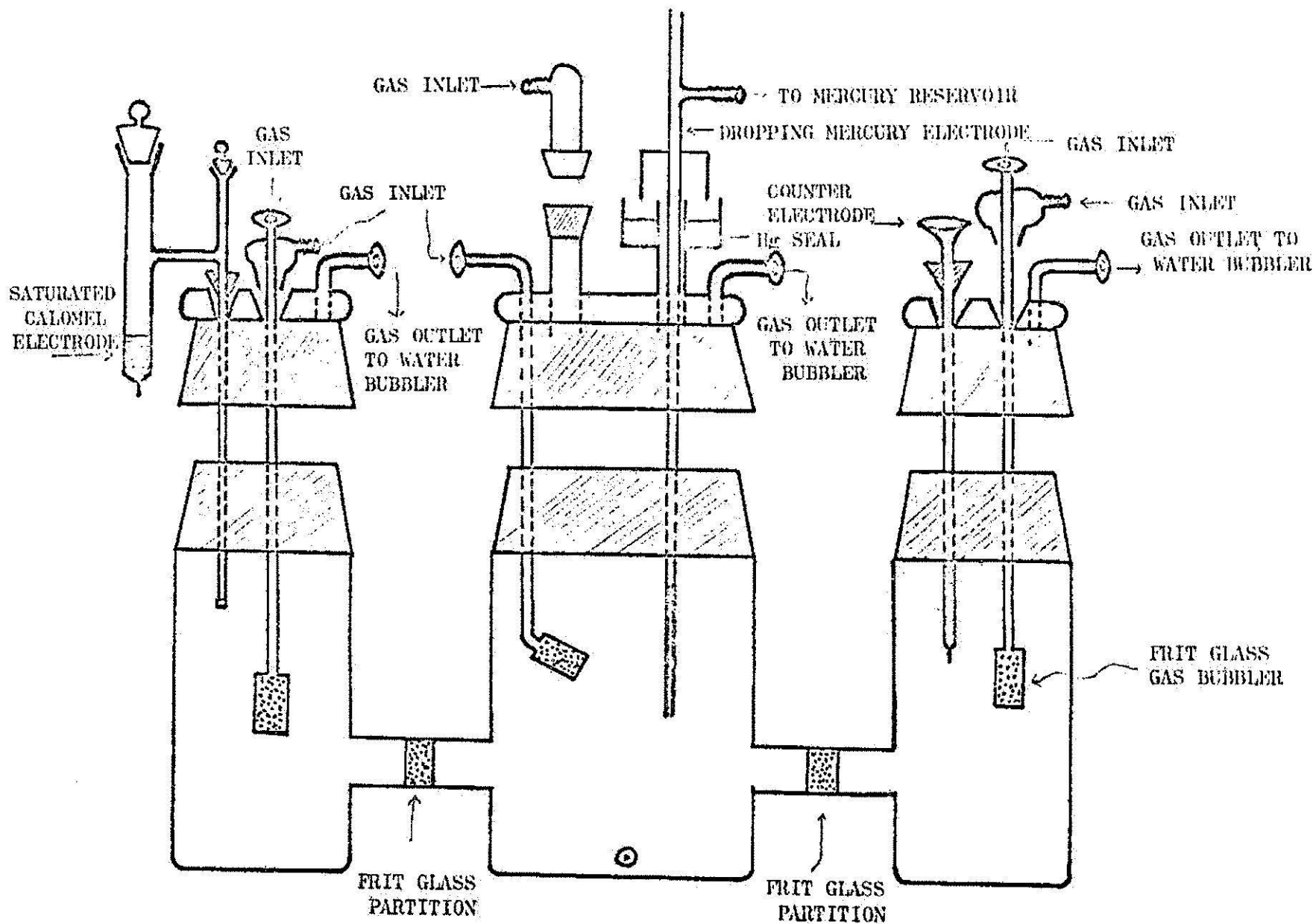
FIG. 5.   ELECTROLYTIC CELL

(iii) Train for the Removal of Oxygen from the Stream of
         Nitrogen:

As the measurements were to be made at very low
concentrations of the electroactive species, oxygen even
in trace amounts was undesirable. The water-pumped
nitrogen supply tank was connected to a combustion tube
filled with pure granulated copper (J.T. Baker, C.P.) by
means of a tygon tube. The combustion tube was placed in
an electrically heated combustion furnace and heated to
about 700° C. The other end of the combustion tube was
connected to a train of five washing bottles with frit-
glass bubblers.   The   second   and   the   third
bottles contained 1M Vanadyl sulfate solution in 20%
sulfuric acid and in contact with amalgamated granulated
zinc at the bottom. Vanadyl solutions had been used by
L. Meites and T. Meites for the effective removal of last
traces of oxygen from nitrogen stream.[31] The first bottle
was left empty in order to accommodate the back-sucked
solution from the subsequent bottles. The fourth bottle
contained triply distilled water so to remove any impurities
picked by the nitrogen from the pervious bottles. In the
fifth bottle, some of the electrolyte under examination
in the main cell was put, so as to maintain the same vapor
pressure above the solution in the cell and above the
solution in the fifth bottle, which was connected to the

cell.

(iv) <u>Constant Temperature Water-Bath</u>: A Sargent Thermonitor Water Bath was used for maintaining a constant temperature of the cell. The cell was placed in the water-bath and all the measurements were made at 25 ± 0.1 $^{\circ}$C.

(v) <u>Recorder</u>: A Sargent #S-72150 Y-t Recorder was used for recording all the measurements. The same recorder was also used for the standardization of the potential applied to the cell (referring to SCE). As I-t curves were desired, the maximum chart speed gears were installed inside the recorder. All the measurements were made at the chart speed of 12 inches per minute.

(vi) <u>Photometric Titrator</u>: Beckman Model B spectrophotometer was converted for use as a photometric titrator as suggested by Goddu and Hume[32, 33]. The sample carriage of the spectrophotometer was removed and the bottom plate of the cell compartment was replaced by a hardboard sheet having two holes. Through the holes, two tygon tubes connected to the inlet and the outlet of a water-driven magnetic stirrer were passed.

The top of the cell compartment was replaced by a

cover modified from a Beckman flame photometric attachment, having a hole just above the beam path of the spectrophotometer. In this hole a rubber stopper with a central hole was fitted. The tip of a 10 ml. precision buret was passed through the central hole of the rubber stopper.

The inside of the cell compartment was painted dull black to make it light-proof. To ensure the complete cut-off of light, the lower part of the buret and the inlet and the outlet tygon tubing were also painted dull black up to about six inches from the holes in the bottom of the cell compartment. The whole arrangement is shown in the Fig. 6.

The Photometric Titrator was used to standardize the vanadyl samples prepared for the study.[25, 26] The complete procedure for standardization will be discussed in experimental procedure.

Chemicals.

(i) Barker Charcoal[34]: About 200 g. of C.P. Charcoal was put in a Soxhlet extractor with glass-wool as a filtering plug. It was refluxed with about 300 ml. of constant boiling hydrochloric acid aqueous mixture for about one month, followed by refluxing with 300 ml. of triply distilled water for about one month, replacing the distalled water periodically, till the filterate was free from chloride ion.

BLACK RUBBER STOPPER

BURET TIP

MONO CHROMATOR CASE

PHOTO TUBE HOUSING

150 ml BEAKER

LIGHT BEAM

STIRRING BAR

MAGNETIC STIRRER

WOODEN PLATFORM

WATER OUTLET (Tygon Tube)

WATER INLET (Tygon Tube)
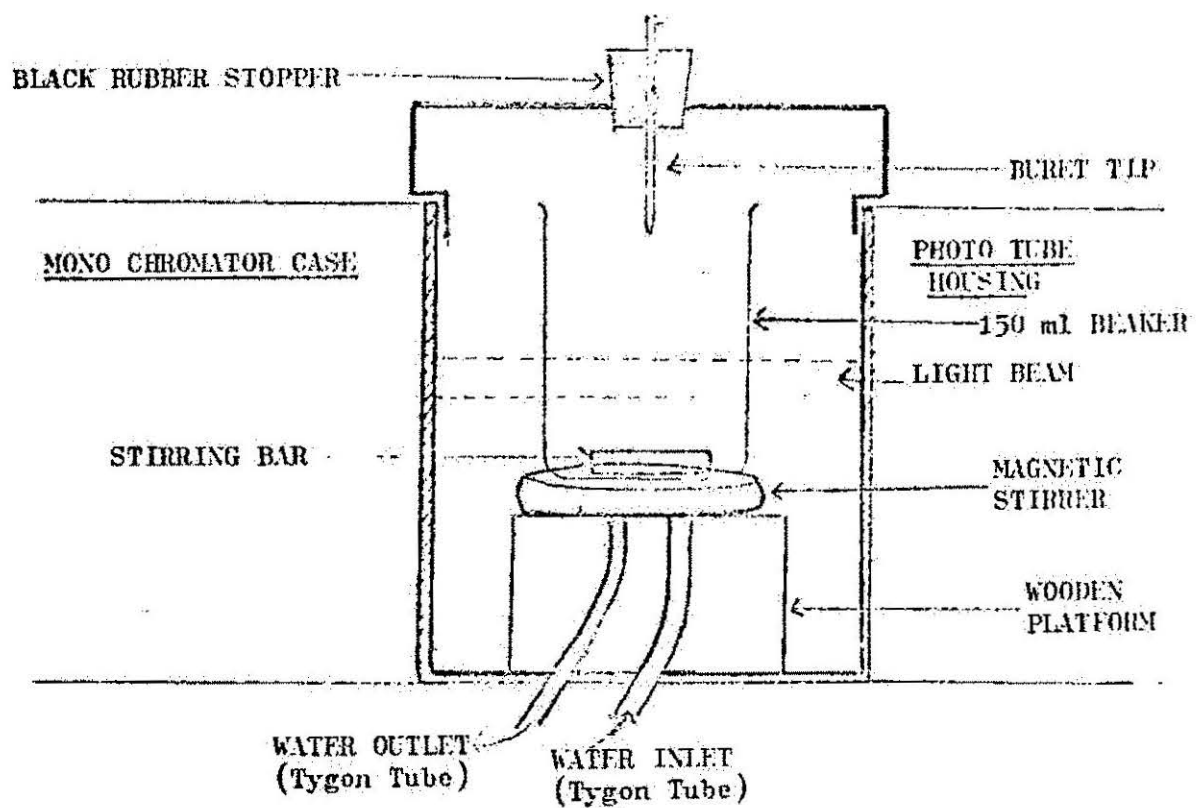
FIG. 6. PHOTOMETRIC TITRATOR

The treated charcoal was dried in an air-heated oven at 140° C., with utmost care to avoid any type of contamination.

All the vanadyl solutions were filtered through the activated charcoal in order to remove any organic suspensions in the solutions.

(ii) Vanadyl Solutions:

(a) Vanadyl Perchlorate VO $(ClO_4)_2$[35, 36, 37]: About 50 g of vanadium pentoxide (Matheson Coleman and Bell, C.P. Grade) was suspended in about 300 ml of triply distilled water and was dissolved by adding 20 ml. of perchloric acid ("Analar," G. Frederick Smith Chemical Co., double vacuum distilled, lead free), to form a yellow solution of VO_2ClO_4. This was reduced to the blue VO $(ClO_4)_2$ by passing sulfur dioxide through the solution. Traces of sulfur dioxide were then expelled by boiling. The resulting solution was filtered through activated charcoal, standardized against potassium permanganate and kept as a stock solution.

(b) Vanadyl Sulfate, $VOSO_4$: This chemical in C.P. grade was acquired from E. H. Sargent Co. No further attempt was made to purify it.

100 ml. of 1M $VOSO_4$ were prepared by dissolving 16.3 g of the sample in triply distilled water. Solution was filtered through the Barker Charcoal and standardized

against potassium permanganate.

(iii) <u>Solutions for Photometric Titration</u>:

(a) <u>Potassium Permanganate Solution</u>: Approximately 0.1M solution was prepared by dissolving about 16 g of $KMnO_4$ of reagent grade (General Chemical Co., New York) in boiling water and allowing the solution to stand overnight. The solution was filtered through a fritted-glass filtering funnel, and standardized against sodium oxalate (reagent grade, primary standard, General Chemical Co., New York) using the Fowler and Bright Method.[38]

(b) <u>Iron (II) Sulfate Solution</u>: (o.1 N $FeSO_4$ in 0.5 % $HClO_4$) "Analar" Grade ferrous sulfate (General Chemical Co., New York) and doubly vacuum distilled perchloric acid were used for preparing this solution.

(c) <u>Ammonium Persulfate Solution</u>: A 15% solution of ammonium persulfate (reagent grade, Baker Chemical Co.) in triply distilled water was prepared.

(iv) Triply vacuum distilled mercury meeting the specification of ACS (Bethlehem Apparatus Co., Hellertown, Pennsylvania) was used in DME.

<u>Experimental Procedure</u>

(i) <u>Photometric Titration</u>: 2 ml. of the vanadyl solution

were taken in a clean 150 ml. beaker.   0.3 ml of H_3PO_4
were added and the sample was reduced with 0.1 NFeSO$_4$ in
0.5 % HC1O$_4$ until a slight excess of Fe^{2+} was shown by an
external ferricyanide spot test.   0.5 ml. of FeSO$_4$ solution
was added in excess.

The spectrophotometer was turned on and allowed to
warm up until the glavanometer was steady.   The sample
beaker containing a magnetic stirring bar was placed in
the path of the light over the magnetic stirrer.   The
monochromater was set to 525 mμ.   0.25 ml of freshly
prepared 15% ammonium persulfate was added.   The stirrer
was turned on and when the solution was homogeneous, the
galvanometer was adjusted to 0.000 optical density.

0.1 ml. aliquot of KMnO$_4$ in the buret was added to
the beaker.   The galvanometer reading was noted when it
reached a constant value.   Another aliquot was added and
the galvanometer reading was noted again.   The process
was repeated till the optical density increased suddenly.
This was the equivalence point.   Several readings on each
side of the endpoint were taken.

The best straight lines between the points taken well
before and after the equivalence point were drawn.   The
point of intersection of the two lines (one before and
one after the equivalence point) was the end point.

A sample plot is given in the Fig. 7.
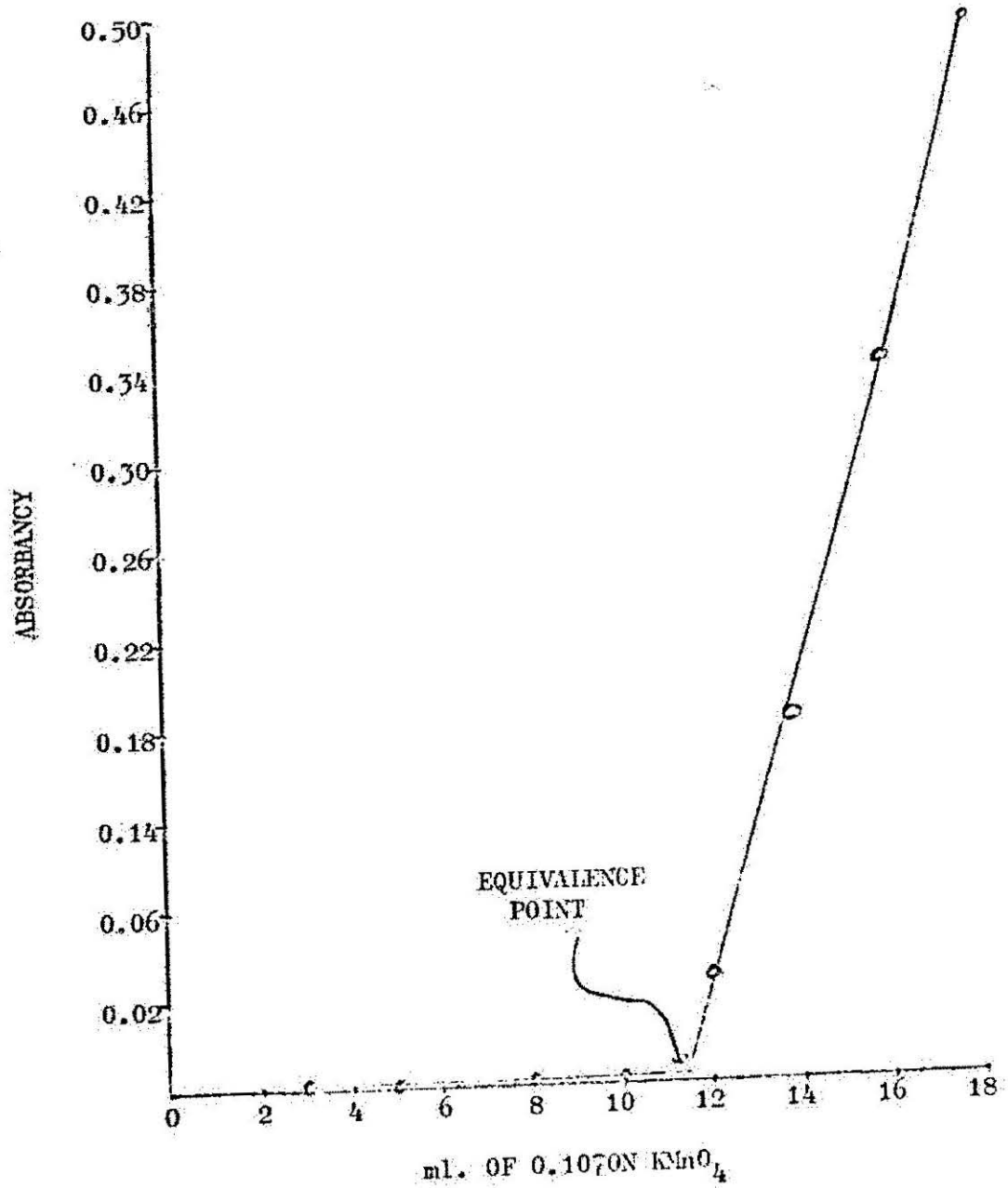
FIG. 7 PHOTOMETRIC TITRATION CURVE

(ii) <u>Amperometry at Constant Potential</u>: (<u>voltammetry at</u>
<u>controlled potential</u>).

(1) All the operational amplifiers, PS-1, PS-2,
recorder and the combustion furnace were turned on.

(2) The cell (Fig. 5) was set in the waterbath
maintained at 25 C.

(3) The test solution was put in all the
compartments of the cell equally distributed (same level).

(4) The cell was connected to the outlet of the
fifth wash-bottle through a three-way stop-cock arrangement.

(5) The nitrogen gas tank was turned on, keeping
the pressure of the gas between 2-3 lbs. per square inch
and letting the gas bubble through the solution by
adjusting the position of the three-way stop-cock.

(6) The solution was deaerated for one hour.
Meanwhile

(7) The recorder was standardized by the procedure
given in the instruction booklet of the recorder.

(8) The recorder position was set to zero after
short-circuiting the positive (red) and negative (black)
input terminals of the recorder by a jumper.

(9) The jumper was removed.

(10) The range knob was turned to 1.25 and units
knob to volts.

(11) The X (output of A5) of the polarographic

circuit was connected to the positive (red) input of the recorder, keeping S_2 in RESET position, S_5 in HOLD position and S_1 in OFF position. The common ground of the circuit was connected to the black terminal of the recorder.

(12) The precision potentiometer R_{14}, was turned till the recorder pen read full scale.

(13) X was disconnected from the positive input of the recorder.

(14) The mercury pool in the central compartment of the cell was connected to the common ground of the main circuit, and the counter electrode to the position X.

(15) The gas stop-cock was adjusted so that the gas passed over the solution.

At this stage, the cathodic reduction of V (IV) took place at the mercury pool in the central compartment. A gradual change in color from blue to blue-violet indicated the reduction.

To ensure the exact equivalence of the V (III) and V (II) concentrations, proceeded as follows:

(16) X was disconnected from the counter electrode (C), and the mercury pool from the ground.

(17) The reference electrode of the cell was connected to R, counter electrode to C and DME to M of the main circuit.

(18) Y was connected to the positive input terminal

of the recorder and the negative terminal of the recorder to the common ground of the circuit.

(19) The Unit knob of the recorder was turned to μA and Range knob to 25, keeping the damping about 50%.

(20) S_1 was turned to ON position.

(21) The Chart Drive was turned to FORWARD, after putting down the pen on the chart.

(22) The switch S_1 and the Chart Drive were turned off after about 1 minute.

(23) The height of the wave (limiting current) was measured from the zero position.

(24) The position of the pen on the chart was adjusted to extreme left by using the Displacement knob. The zero-line was marked.

(25) The switch S_4 was thrown to the other side (polarity change).

(26) The steps (20), (21), (22) and (23) were repeated. The limiting currents measured in steps (23) were equal on changing the polarity of S_4, so the reduction was to the desired stage (exact equivalence of V (III) and V (II). Amperometry at constant potential was performed as follows:

(27) X was connected to the positive terminal of the recorder, keeping the negative terminal of the recorder connected to the common ground of the circuit.

(28) The Unit knob was turned to mv and the Range knob to 250.

(29) The potentiometer R_{14} was turned till the recorder pen read zero.

(30) X was disconnected from the positive terminal of the recorder.

(31) Y was connected to the positive terminal of the recorder and Unit knob was turned to μA with Range at 50.

(32) S_1 was turned to ON position.

(33) The chart drive knob was turned to FORWARD after putting down the recorder pen on the chart.

The recorder gave the plot of I-t for the individual mercury drops of DME at zero potential.

(34) The steps (27) to (33) were repeated by setting the potentiometer R_{14} for 100 mv, 200 mv...etc. (each setting with an increment of 100 mv).

(35) The process was repeated as in step (34), after changing the polarity of the PS-1 by throwing the switch S_4 to the other side.

CHAPTER IV

DATA AND DISCUSSION

Figure 8 shows the plots of electrocapillary curves of Hg-1M $HClO_4$ and Hg-varying molar concentrations of V(III)/V(II) in 1M $HClO_4$ interfaces. The concentration of the couple is expressed as molar concentration of the salt of one of the components of the couple, $V(ClO_4)_3$. The concentrations of $V(ClO_4)_3$ are 0.005M, 0.010M and 0.050M for the curves top to bottom respectively. The relevant data is given in Tables II-VI.

In the third column of Tables III-V, γ values have been calculated from drop-time t, by multiplying t with 1.086×10^2.

The fourth column in Tables III-V refers to the slope of the electrocapillary curves at a particular potential shown in the E^- column. The $\left(\frac{\partial \gamma}{\partial E^-}\right)$ values are in appropriate units of charge (μ coulomb per square centimeter) in order to use them directly in the equation

$$\left(\frac{\partial \gamma}{\partial E^-}\right)_{T,p,\mu's} = -\left(q^M - \Gamma_{i,u}^{z_i}\right)F$$

Column five shows the intercept A, on $It^{1/3}$ axis in the plot of $It^{1/3}$ vs $t^{\frac{1}{2}}$ (page 61). The measurements of I have been made from potentiostat controlled Current-Time (I-t) curves of a single drop. In the Fig. 9, sample I-t

curves for anodic as well as cathodic side along with
relevant sample $It^{1/3}$ vs $t^{\frac{1}{2}}$ plots are shown. The best
fitting straight lines were drawn using the method of
least squares. The value of q^M shown in the sixth column
of the above tables has been determined from A by the
relationship

$$q^M = \frac{A}{3.22} \left(\frac{\rho_{H_2}}{n} \right)^{\frac{2}{3}} = \frac{A}{3.22} \left(\frac{13.533}{0.002137} \right)^{\frac{2}{3}}$$

In Table VI, Column 3, $a_{V(ClO_4)_3}$ has been computed by
applying Debye-Huckel limiting law (EDHL).

From the slope of γ-lna plots, the value of F/RT .
$(\frac{\partial \gamma}{\partial \ln a})$ in units of charge can be calculated.

The plots in Fig. 8 have the general shape of a para-
bola. As E changes from positive to more negative values,
γ first increases (ascending branch), then passes through
an electrocapillary maximum (ECM) and finally decreases
(descending branch). Column 6 of Tables III-V, shows that
the value of q^M is positive on the ascending branch of the
electrocapillary curves and decreases as E becomes more and
more negative. On the descending branch, q^M becomes negative
and its magnitude increases negatively with increasing
negative E^-. At the electrocapillary maximum (ECM) the
value of q^M is zero. This point of zero charge (PZC)
corresponds to -0.525, -0.440, -0.425, and -0.350 volts
for the various concentrations in the Figure 8. It is noted
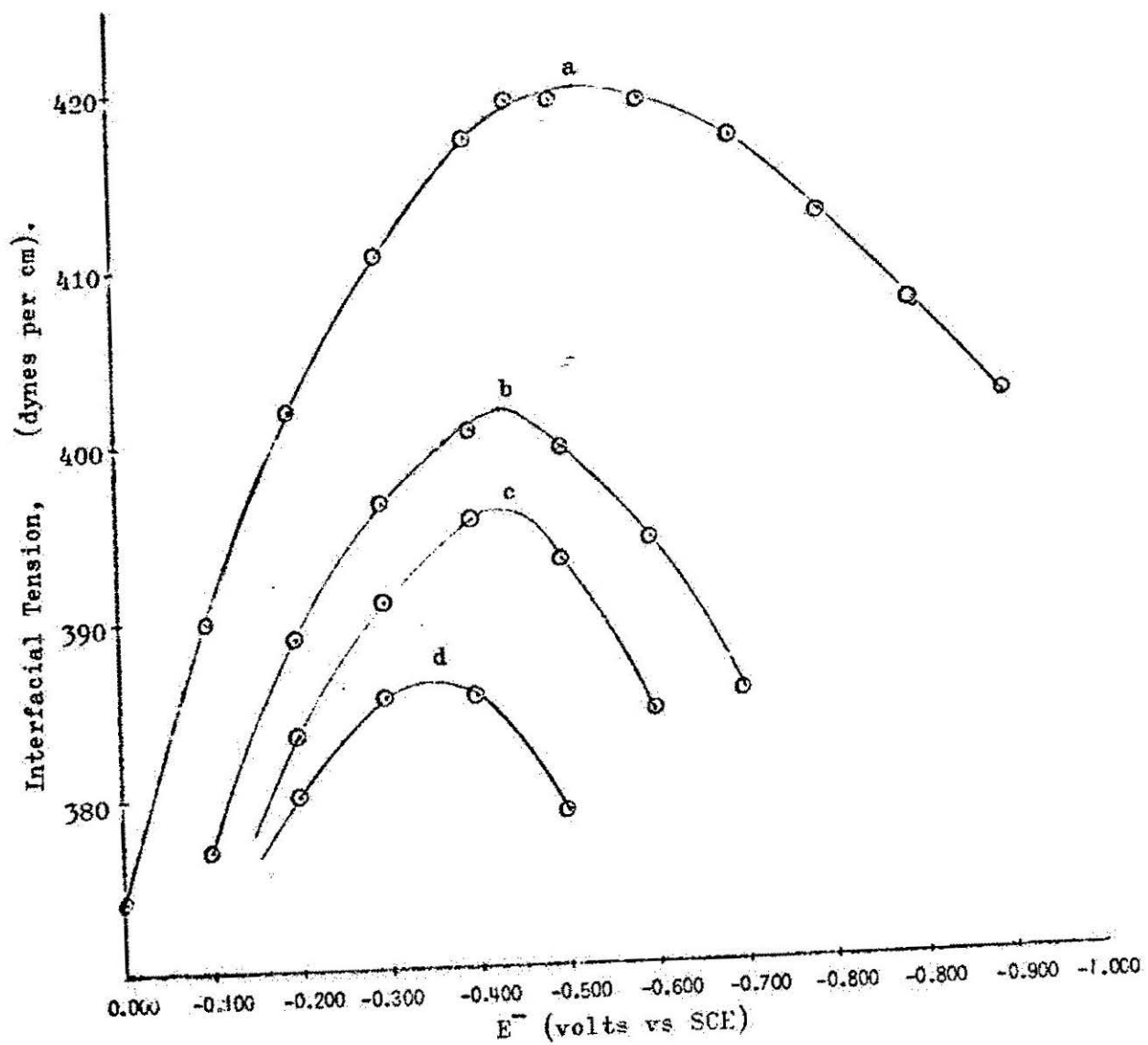
FIG. 8. Electrocapillary Curves for Interfaces:

(a) Hg-1M HClO$_4$

(b) Hg-0.005M V(ClO$_4$)$_3$ in 1M HClO$_4$

(c) Hg-0.010M V(ClO$_4$)$_3$ in 1M HClO$_4$

(d) Hg-0.050M V(ClO$_4$)$_3$ in 1M HClO$_4$
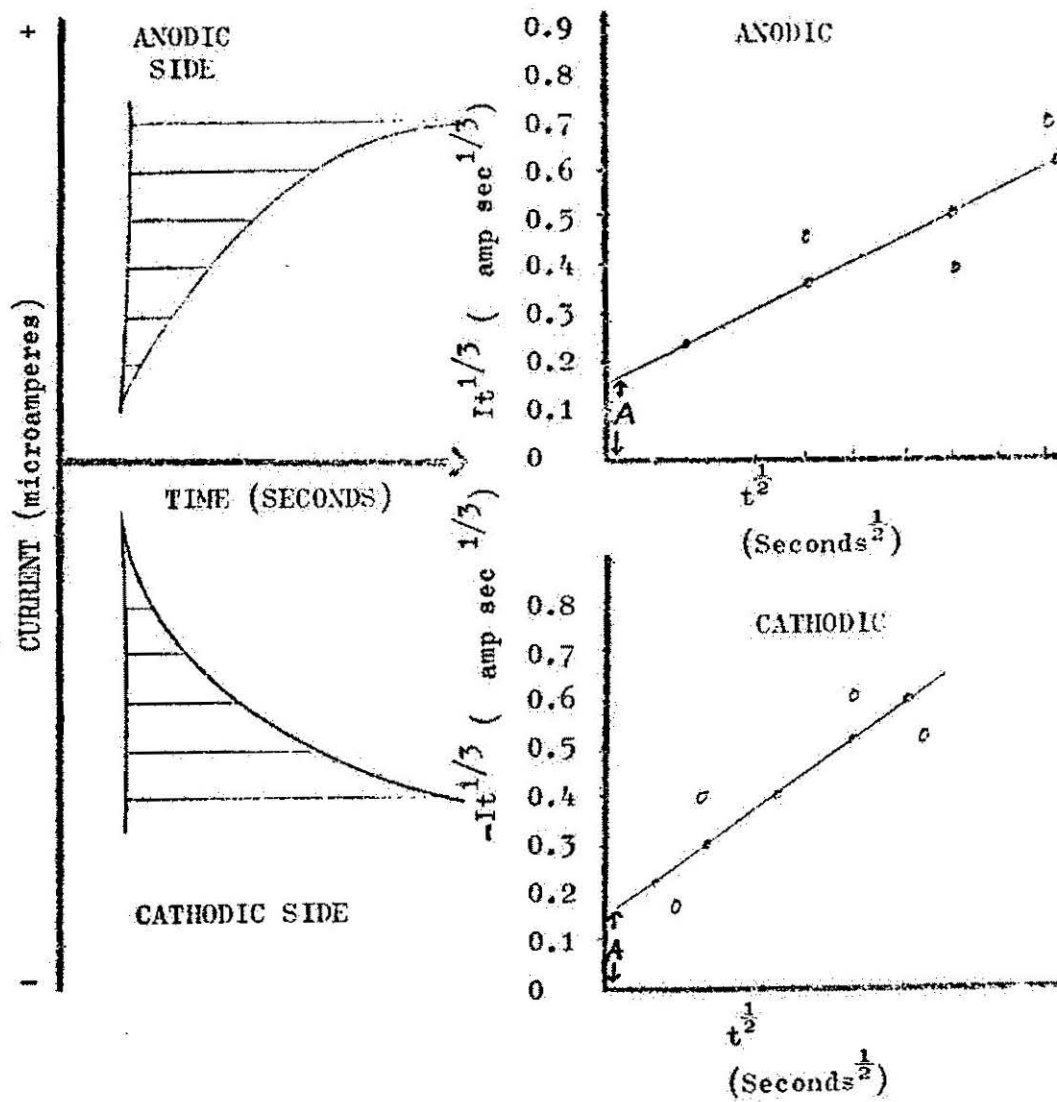
FIG. 9. I-t and $It^{1/3}-t^{\frac{1}{2}}$ PLOTS

TABLE II

ELECTROCAPILLARY DATA FOR Hg and 1M $HClO_4$

E^- volts (vs SCE)	Drop-Time, t (seconds)	Interfacial Tension, γ (dynes per cm.)
-0.000	3.45	374.6
-0.100	3.59	389.8
-0.200	3.70	401.8
-0.300	3.78	410.6
-0.400	3.84	417.0
-0.450	3.86	419.2
-0.500	3.86	419.2
-0.600	3.86	419.2
-0.700	3.84	417.0
-0.800	3.80	412.6
-0.900	3.75	407.2
-1.000	3.70	401.8

TABLE III

ELECTROCAPILLARY AND DOUBLE LAYER DATA FOR

Hg and 0.005M VANADIC PERCHLORATE IN 1M $HClO_4$

E^-	t	γ	$\left(\dfrac{\partial \gamma}{\partial E^-}\right)_{T,h,\mu_2}$	A	q^M	$F\Gamma_{V,\omega}^{2+}$
-0.100	3.47	377.0	10.00	0.191	20.24	30.24
-0.200	3.57	388.0	10.00	0.097	10.28	20.28
-0.300	3.65	396.4	6.82	0.040	4.24	11.06
-0.400	3.69	400.7	1.48	0.012	1.27	2.75
-0.500	3.68	399.6	-4.28	-0.017	-1.80	-6.08
-0.600	3.63	394.2	-6.25	-0.063	-6.68	-12.93
-0.700	3.55	385.5	-9.00	-0.116	-12.29	-21.29

$E^- =$ potential of DME (volts vs SCE),

$t =$ drop time in seconds, $\gamma =$ interfacial

tension in dynes per cm., A = intercept on

$It^{1/3}$ axis, $q^M =$ charge density per cm^2 on

the electrode, $F\Gamma_{V,\omega}^{2+} =$ surface excess of v^{2+}

relative to water in units of charge.

$\left(\dfrac{\partial \gamma}{\partial E^-}\right)$ expressed in units of charge

density.

TABLE IV

ELECTROCAPILLARY AND DOUBLE LAYER DATA FOR

Hg and 0.010M VANADIC PERCHLORATE IN 1M $HClO_4$

E^-	t	γ	$\left(\dfrac{\partial \gamma}{\partial E^-}\right)_{T,\mu,H'}$	A	q^M	$F\Gamma_{V,\omega}^{2+}$
-0.200	3.53	383.3	8.30	0.119	12.61	20.91
-0.300	3.60	390.9	5.00	0.057	6.04	11.04
-0.400	3.64	395.3	3.07	0.014	1.48	4.55
-0.500	3.62	393.1	-6.66	-0.049	-5.19	-11.85
-0.600	3.54	384.4	-8.33	-0.107	-11.34	-19.67

E^- = potential of DME (volts vs SCE), t = drop time in seconds, γ = interfacial tension in dynes per cm., A = intercept on $It^{1/3}$ axis, q^M = charge density per cm^2 on the electrode.

$F\Gamma_{V,\omega}^{2+}$ = surface excess of V^{2+} relative to water in units of charge, $\left(\dfrac{\partial \gamma}{\partial E^-}\right)$ expressed in units of charge density.

TABLE V

ELECTROCAPILLARY AND DOUBLE LAYER DATA FOR Hg AND 0.050M VANADIC PERCHLORATE IN 1M $HClO_4$

E^-	t	γ	$\left(\dfrac{\partial \gamma}{\partial E^-}\right)_{T,p,\mu}$	A	q^M	$F\Gamma_{V,w}^{2+}$
-0.200	3.50	380.1	10.00	0.145	15.37	25.37
-0.300	3.55	385.5	5.00	0.071	7.52	12.52
-0.400	3.55	385.5	-4.28	-0.072	-7.63	-11.91
-0.500	3.49	379.0	-8.75	-0.155	-16.43	-25.18

E^- = potential of DME (volts vs SCE), t = drop time in seconds, γ = interfacial tension in dynes per cm, A = intercept on It$^{1/3}$ axis q^M = charge density per cm^2 on the electrode, $F\Gamma_{V,w}^{2+}$ = surface excess of V^{2+} relative to water in units of charge, $\left(\dfrac{\partial \gamma}{\partial E^-}\right)$ expressed in units of charge density.

TABLE VI

DATA FOR RELATIVE SURFACE EXCESS OF $V(ClO_4)_3$

E^-	Concentration (Molar)	$\ln a_{V(ClO_4)_3}$	$F/RT\left(\frac{\partial\gamma}{\partial\ln a}\right)_{E^-}$	$F\Gamma_{V^{3+},\omega}$
-0.200	0.005	-8.875	54.60	34.32
	0.010	-8.295	22.23	1.32
	0.050	-7.266		-25.37
-0.300	0.005	-8.875	50.70	39.63
	0.010	-8.295	31.98	20.94
	0.050	-7.266	16.38	28.90
-0.400	0.005	-8.875	37.44	34.69
	0.010	-8.295	37.44	32.89
	0.050	-7.266	37.44	49.35
-0.500	0.005	-8.875	47.34	53.42
	0.010	-8.295	47.34	59.19
	0.050	-7.266	47.34	72.52

$E^- =$ potential of DME (volts vs SCE), $F/RT\left(\frac{\partial\gamma}{\partial\ln a}\right)$ and $F\Gamma_{V^{3+},\omega}$ in units of charge.

that the point of zero charge is shifted towards more positive potentials as the concentration of the V(III)/V(II) couple is increased. Esin and Markov have mentioned that the shifting of point of zero charge is due to ionic adsorption on the electrode (Esin-Markov Effect).[39] Frumkin and coworkers have noted this type of behavior in their study of cathodic reduction of $TlNO_3$.[40-43] They showed by analysis of the electrocapillary curves (Fig. 10) that Tl^+ ions are strongly adsorbed on mercury and this conclusion is confirmed by kinetic study of the discharge of Tl^+ ions on the thallium amalgam.[44,45] On the same basis we can say that there is a strong cationic adsorption in the system under investigation. This fact is further confirmed by the positive relative surface excesses of V^{3+} and V^{2+} (i.e. $F\Gamma_{V,\omega}^{II}$ and $F\Gamma_{V,\omega}^{II}$) on the anodic branch of the electrocapillary curves (column 7 in Tables III-V and Column 5 in table VI). The relative surface excess is a sort of quanitiative measure of adsorption.

The above fact appears somewhat surprising at first glance, for it would be natural to suppose that on the left side of the ECM, where q^M is positive, cations (V^{+3} and V^{+2}) would be repelled away from the interface and that $F\Gamma_{V,\omega}^{II}$ and $F\Gamma_{V,\omega}^{II}$ would be therefore negative. The detailed nature of the forces of interaction between an ion and the metal surface which bring about specific adsorption has not yet
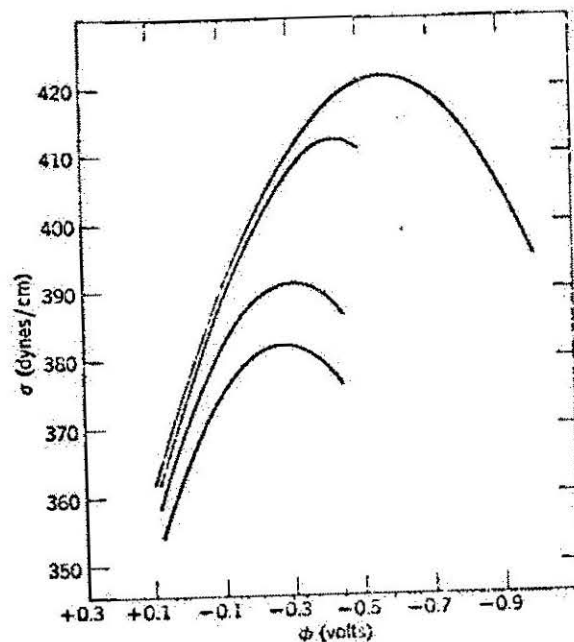
Figure 10. Electrocapillary curves of mercury in
1N KNO_3 + 0.01N HNO_3 + $xTlNO_3$ vs. N.C.E. Curves
from top to bottom: x = 0; 0.01N; 0.1N; 0.2N.
[Frumkin (27)]
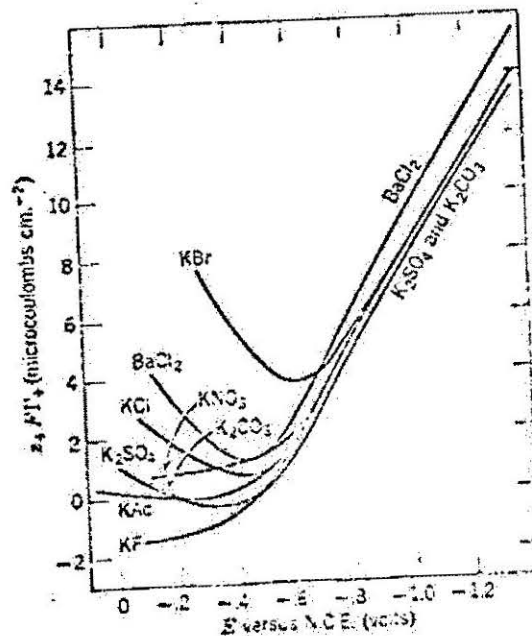

Figure 11. Relative (to water) surface excesses of
cations for mercury in 0.1 normal solutions of different
electrolytes at 25°C. Surface excess expressed as a
charge [Grahame and Soderberg (46)]

been wholly resolved. The best explanation which seems capable of accounting for this behavior is specific adsorption of the anion (ClO_4^-). That is, there must be some kind of additional, non-coulombic interaction between ClO_4^- ions into the double layer than that which can be accounted for by simple coulombic attraction. This super-equivalent (to q^M) quantity of perchlorate ion then attracts sufficient additional V^{3+} and V^{2+} ions (counter ions) to maintain the electroneutrality of the entire interfacial region, that is, to make $q^s = -q^M$. As q^M becomes more positive, the amount of specifically adsorbed ClO_4^- ions increases and this increase is reflected in an increased positive adsorption of V^{3+} and V^{2+} counterions. Studies of Grahame and Soderberg in this connection are worth mentioning.[46] Fig. 11 shows their results regarding cationic adsorption. It is noticed in the figure that $\sum_+ F\Gamma_+$ is always positive for all cations and increases with q^M. Though $F\Gamma_{V,3+}$ remains positive on both sides of the point of zero charge (except on extreme anodic side and at higher concentration of the $V(III)/V(II)$ couple), the value of $F\Gamma_{V,2+}$ is negative on the cathodic branch of the electrocapillary curves. This fact can be explained by considering the preferential adsorption of V^{3+} at potentials more negative than PZC due to greater positive charge on V^{3+} than that on V^{2+}. The nature of this adsorption is coulombic than specific. Abnormally

high $F_{V,\omega}$ values (Table VI-column 5) confirm this view.

At extreme anodic and cathodic potentials, the drop-time becomes almost constant and the limiting current values for anodic oxidation and cathodic reduction respectively are reached, thus confining the electrocapillary measurements near the equilibrium potential of the redox couple. The electrocapillary curves around the equilibrium position are symmetrical. V(III)/V(II) studies in 0.5M H_2SO_4 were also attempted, but too much scatter of the drop time (hence γ) was observed; due probably to non-electroactive impurities in H_2SO_4. As the accuracy of such measurements was doubtful, no attempt has been made to analyze the data. Tables VII and VIII and Fig. 12 pertain to this system.

TABLE VII

ELECTROCAPILLARY DATA FOR Hg AND 0.5M H_2SO_4

E⁻ volts (vs SCE)	Drop-time, t (seconds)	Interfacial Tension, γ (dynes per cm.)
0.000	3.45	380.0
-0.100	3.68	400.5
-0.200	3.75	408.0
-0.300	3.82	414.0
-0.400	3.85	419.0
-0.500	3.86	419.5
-0.700	3.83	416.0
-0.800	3.80	413.5
-0.900	3.77	409.0
-1.000	3.72	403.5

TABLE VIII

ELECTROCAPILLARY DATA FOR Hg AND VARIOUS CONCENTRATIONS OF $V_2(SO_4)_3$ IN 0.5M H_2SO_4

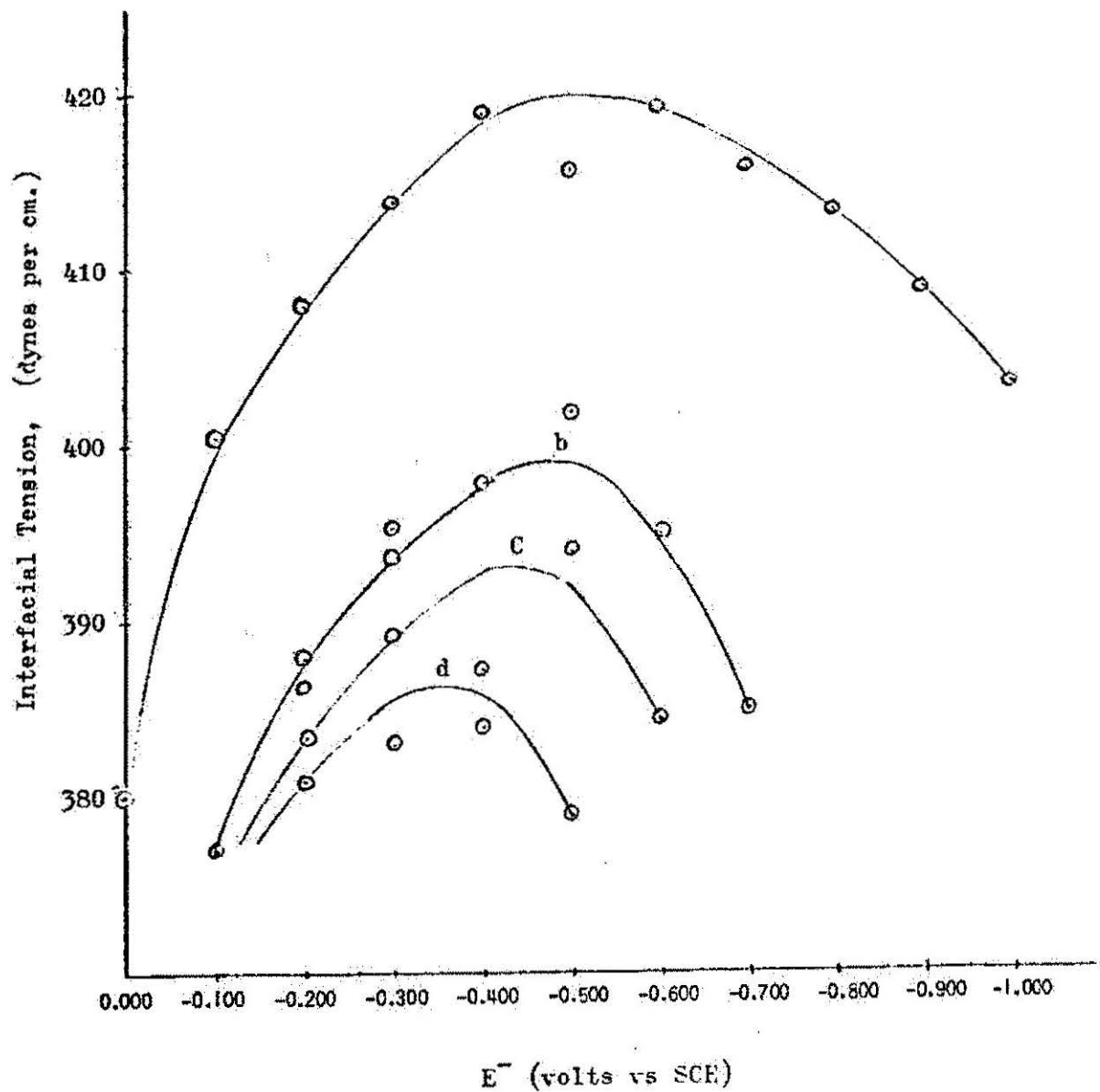| E^-	0.0025M		0.0050M		0.0250M	
	t	γ	t	γ	t	γ
-0.100	3.47	377.0	--	--	--	--
-0.200	3.57	388.0	3.53	383.5	3.50	381.0
-0.300	3.62	393.5	3.58	389.0	3.53	383.0
-0.400	3.67	398.0	--	--	3.54	384.0
-0.500	3.70	402.0	3.63	394.0	3.48	379.0
-0.600	3.64	395.0	3.55	384.5	--	--
-0.700	3.55	385.5	--	--	--	--

FIG. 12. Electrocapillary Curves for Interfaces:

(a) $Hg-0.5M\ H_2SO_4$

(b) $Hg-0.0025M\ V_2(SO_4)_3$ in $0.5M\ H_2SO_4$

(c) $Hg-0.0050M\ V_2(SO_4)_3$ in $0.5M\ H_2SO_4$

(d) $Hg-0.0250M\ V_2(SO_4)_3$ in $0.5M\ H_2SO_4$

CHAPTER V

CONCLUSION

In the foregoing pages, the theory of electrocapillarity was put into new perspective and an attempt was made to apply the theory to a charge transfer electrode. Little is known in this respect and the test of the theory rests on speculation. However, using a fast response and stable potentiostat built in this laboratory, coupled with a sensitive recorder, an attempt has been made to be as accurate as possible and to give a quantitative picture of the double layer in terms of the surface excesses of the oxidant and the reductant of the redox couple constituting the charge transfer electrode. The values of excess of charge density on the electrode q^M, another parameter of the electrical double layer, have also been reported. Such data have never been reported due to lack of sophistication in instrumentation and the complex nature of the electrode processes.

In the present investigation, the analysis of I-t curves has been done taking into consideration the composite nature of the process involved; faradaic and non-faradaic. The values of q^M have been calculated from the double layer charging current instead of taking the derivative $\left(\frac{\partial \gamma}{\partial E^-}\right)_{\mu_i}$

as a measure of q^M as has been previously done in the case
of non-faradaic processes, thus accounting for faradaic
processes as well.

The importance of the double layer structure in the
interpretation of the kinetics of an electrode reaction was
first pointed by Frumkin[47] in 1933. Much interest has been
shown recently in such studies by other investigators.[48-51]
The structure of the double layer at an electrode-electrolyte
interface affects the kinetics of electrochemical reactions
for two reasons: (a) the concentrations of ionic reactants
are not the same at the reaction site (OHP) as in the bulk
of the solution, (b) the effective difference of potential
must be corrected for the difference of potential across
the diffuse double layer (i.e., $\phi_2 - \phi_s$ and not $\phi_M - \phi_s$).

In the present investigation, the relative surface
excesses of ions ($\Gamma_{V,\omega}^{2+}$ and $\Gamma_{V,\omega}^{3+}$) are the measure of excess
of concentration of ions at OHP over that in the bulk of the
solution. The value of ($\phi_2 - \phi_s$) can be calculated by
the method outlined by Mohilner[22] by using q^M, $\Gamma_{V,\omega}^{2+}$ and $\Gamma_{V,\omega}^{3+}$
values.

The potential difference ($\phi_2 - \phi_s$) and the surface
excesses can be further utilized to calculate the kinetic
parameters such as transfer coefficient α, standard
rate constants k_s, heat of activation at standard potential
$\Delta H_s^{\ddagger}$ etc., giving data corrected for double layer effects.

Relaxation techniques such as potentiostatic or galvanostatic can be applied for this purpose as described by Delahay.[52]   Similar data <u>without</u> double layer correction have been recently published by Tanaka and Tamamushi.[53] They have pointed out the importance of α and k values in electrode kinetics and the experimental difficulties involved in getting them.

This investigation may be considered as a preliminary step towards the kinetic study of the charge transfer reversible reaction V(III)/V(II).   It has outlined the theory of electrocapillarity of a redox electrode and has given a quantitative picture of the double layer structure in presence of electro-active species. Techniques and methods for obtaining the double layer adsorption parameters have been developed.

Solvent interaction and complex formation should be further investigated and equations like (61) and (62) can be developed and tested through experimentation.

BIBLIOGRAPHY

(1) H. L. F. von Helmholtz, Ann. Physik. (2) 89, 211 (1853).

(2) G. Quinke, Ann. Physik. (2) 113, 513 (1861).

     "   "   Pogg. Ann., 113, 513 (1861).

(3) D. L. Chapman, Phil. Mag. 6, 25, 475 (1913).

(4) G. Gouy, J. Phys. radium, (4) 9, 457 (1910).

     "   "   comp. rend., 149, 654 (1910).

     "   "   Ann. Phys., Paris, 7, 163 (1917).

(5) O. Stern, Z. Elektrochem, 30, 508 (1924).

(6) D. C. Grahame, Chem Rev., 41, 441 (1947).

     "   "   "   A. Elektrochem, 59, 773 (1955).

     "   "   "   J. Chem Phys., 21, 1054 (1953).

     "   "   "   J. Am. Chem. Soc., 76, 4819 (1954).

     "   "   "   J. Am. Chem. Soc., 79, 2093 (1957).

     "   "   "   J. Am. Chem. Soc., 68, 301 (1946).

     "   "   "   J. Chem. Phys., 18, 903 (1950)

     "   "   "   J. Chem. Phys., 21, 1054 (1953).

(7) J. R. Macdonald, J. Chem. Phys., 22, 1857 (1954).

(8) J. R. Macdonald, C. A. Barlow, J. Chem. Phys., 36, 3062 (1962).

(9) R. B. Whitney and D. C. Grahame, J. Chem. Phys., 9, 827 (1941).

(10) D. C. Grahame, Proc. 3rd Meeting CITCE, Berne, 1951, Carlo-Manfredi - Editore, Milan, 1952, pp. 330-345.

(11) M. A. V. Devanathan, Trans. Faraday Soc., 50, 373 (1954).

(12) J. O'M Bockris, M. A. V. Devanathan, K. Müller, Proc. Roy. Soc. (London) A274, 55 (1963).

(13) D. C. Grahame, R. B. Whitney, J. Am. Chem. Soc., 64, 1548 (1942).

(14) R. Parsons, and M. A. V. Devanathan, Trans. Faraday Soc., 49, 404 (1953).

(15) B. E. Conway, "Electrode Processes," p. 62, Ronald Press, New York, 1965.

(16) R. Parsons, "Equilibrium Properties of Electrified Interphases," in Modern Aspects of Electrochemistry, No. 1, (J. O'M. Bockris, Ed.), Butterworths, London, 1954, Chap. 3.

(17) P. Van Rysselberghe, Electrochemical Affinity (No. 1237 in the series, Actualities Scientifiques et Industrielles), Hermann, Paris, 1955.

(18) R. Parsons, Trans. Faraday Soc., 51, 1518 (1955).

(19) E. A. Guggenheim, Trans. Faraday Soc., 36, 397 (1940).

(20) F. O. Koenig, J. Phys. Chem., 38, 339 (1934).

(21) D. C. Grahame and R. B. Whitney, J. Am. Chem. Soc., 64, 1548-1552 (1942).

(22) D. M. Mohilner, J. Phys. Chem., 66, 724 (1962).

(23) M. A. V. Devanathan, Chem. Rev., 65, 635-684 (1965).

(24) D. C. Grahame and R. B. Whitney, J. Am. Chem. Soc., 64, 1548 (1942).

(25) F. O. Koenig, W. H. Wohlers and D. Bandini, Abstracts, CITCE meeting, Moscow, 1963.

(26) M. Sluyters, Rehbach, W. J. A. Woitteiz, J. H. Sluyters, J. Electroanal. Chem., 13, 31-34 (1967).

(27) A. Frumkin, Trans. Symposium on Electrode Process, Philadelphia (1961), pp. 1-16, John Wiley and Sons Inc., New York.

(28) J. N. Butler and Mary L. Meehan, J. Phys. Chem. 69, 4051 (1965).

(29) G. L. Booman and W. B. Holbrook, Anal. Chem., 37, 795 (1965).

(30) R. G. Barradas and J. L. A. French, Anal. Chem. 39, 1037 (1967).

(31) L. Meites and T. Meites, Anal. Chem., 20, 984 (1948).

(32) Goddu, R. F., and Hume, D. N., Anal. Chemistry 26, 1679 (1954).

(33) Goddu, R. F., and Hume, D. N., Anal. Chemistry 26, 1740 (1954).

(34) G. Barker, Square Wave Polarography, Part 3, Atomic Energy Research Establishment, Harwell, 1957.

(35) K. M. Joshi, Wolfgang Mehl, R. Parsons, Trans. Symp. on Electrode Process, Philadelphia, pp. 249 (1961) John Wiley and Sons.

(36) Grinnell Jones and John Henry Colvin, J. Am. Chem. Soc., 66, 1563-1571 (1944).

(37) Grinnell Jones and John Henry Colvin, J. Am. Chem.
      Soc., 66, 1572 (1944).

(38) Fowler and Bright, Prod., J. Research Nat'l. B.S.,
      15, 493 (1935).

(39) Esin, O. A. and B. F. Markov, Acta Physiochem., URSS
      10, 353 (1939).

(40) A. N. Frumkin and A. S. Titievskaja, Zhur. Fiz. Khim.
      31, 485 (1957).

(41) A. N. Frumkin and N. S. Polyanovskaya, Zhur. Fiz.
      Khim. 32, 157 (1958).

(42) A. N. Frumkin, Surface Phenomena in Chemistry and
      Biology, J. F. Danieli, K. G. A. Parkhurst and A. C.
      Riddiford, editors, Pergamon Press, London, 1958,
      pp. 189-194.

(43) A. N. Frumkin, Transactions of the Symposium on
      Electrode Processes, E. Yeager Editor, John Wiley,
      New York, 1961 pp. 1-12.

(44) G. C. Barker, Transactions of the Symposium on
      Electrode Processes, E. Yeager editor, John Wiley,
      New York, 1961 (pp. 325-365).

(45) M. Rehbach and J. H. Sluyters, Rec. trav. chim, 80,
      469 (1961). Rec. trav. chim. 81, 301 (1962).

(46) D. C. Grahame, and B. A. Soderberg, J. Chem. Phys.
      22, 449 (1954).

(47) A. N. Frumkin, Z. physik. Chem. 164, 121 (1933) For

extensive review, Z. Elektrochem; <u>59</u>, 807 (1955).

(48)   M. Brieter, M. Kleinerman and P. Delahay. J. Amer.
Chem. Soc., <u>80</u>, 5111 (1958).

(49)   L. Griest, "cinetique d'approche et reactions
d'electrodes irréversible," University of Brussels,
(1958).

(50)   L. Griest, Trans: of the Symposium on Electrode
Processes, Philadelphia, pp. 109, John Wiley & Sons
(1961).

(51)   W. H. Reinmuth, L. B. Rogers and L. E. I. Hummelstedt,
J. Amer. Chem. Soc., <u>81</u>, 2947 (1959).

(52)   P. Delahay, Advances in Electrochemistry and Electro-
chemical Engineering, eds. P. Delahay and C. W. Tobias,
Vol. I. pp. 233, John Wiley & Sons (1961).

(53)   N. Tanaka and R. Tamamushi, Electrochimica Acta, <u>2</u>,
963 (1964).

(54)   I. Lanmuir, Trans. Faraday Soc., <u>17</u>, 641 (1924).